JRRD Guest Editorial

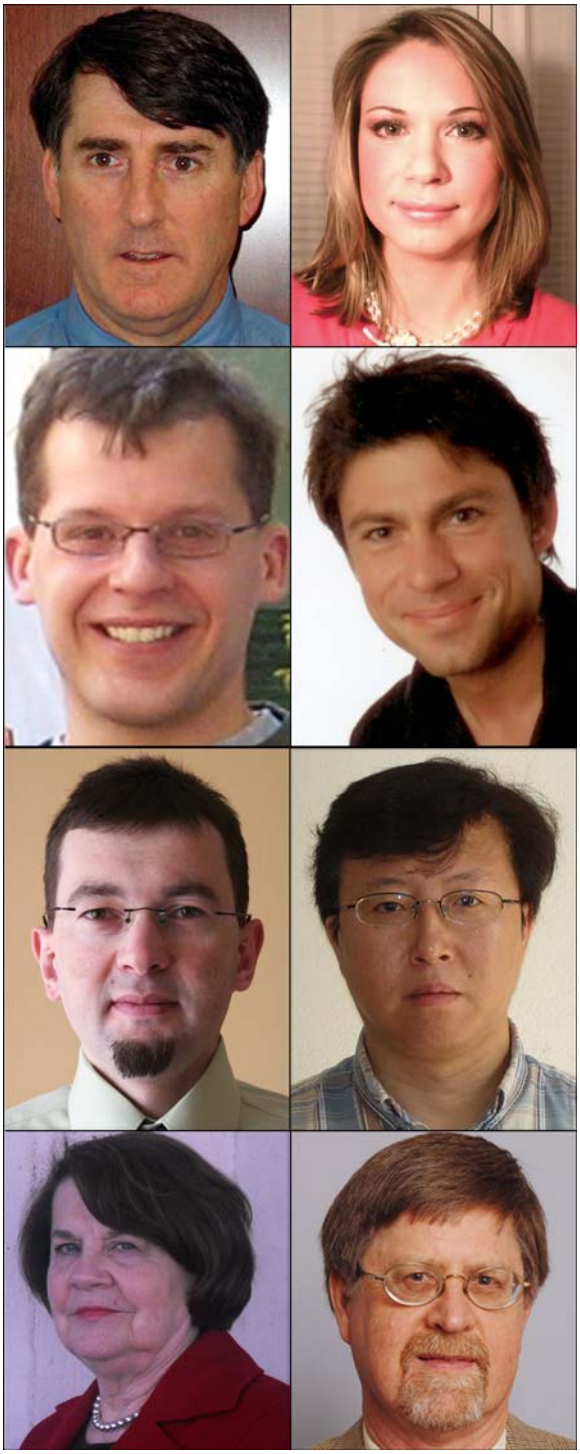

Bruce Crosson, PhD; Anastasia Ford, BS; Keith M. McGregor, PhD; Marcus Meinzer, PhD; Sergey Cheshkov, PhD; Xiufeng Li, PhD; Delaina Walker-Batson, PhD; Richard W. Briggs, PhD

Functional imaging and related techniques: An introduction for rehabilitation researchers

Over the past 25 years, techniques to image brain structure and function have offered investigators in the cognitive neurosciences and related fields unprecedented opportunities to study how human brain systems work and are connected. Indeed, the number of peer-reviewed research articles using these techniques has grown at an exponential rate during this period. Inevitably, investigators have become interested in mapping neuroplastic changes that support learning and memory using functional neuroimaging, and concomitantly, rehabilitation researchers have become interested in mapping changes in brain systems responsible for treatment effects during the rehabilitation of patients with stroke, traumatic brain injury, and other brain injury or disease. This new rehabilitation research and development arena is important because a greater understanding of how and why brain systems remap in the service of rehabilitation will lead to the development of better treatments.

At the same time that functional neuroimaging methods have been developed, new structural neuroimaging techniques have also been added to the toolbox of rehabilitation researchers. For example, diffusion tensor imaging (DTI) and related magnetic resonance (MR)* techniques offer the ability to assess human white-matter pathways in vivo. Not only can these techniques be used to estimate the integrity of a given volume of white matter, but they can also be used to trace fiber tracts within the brain. This latter development is exciting because most of what we know (or at least thought we knew) about the connections of the human cortex has actually come from research on nonhuman primates, leaving questions especially about the phylogenetically newer portions of the cortex. In the rehabilitation arena, a better understanding of how the brain's connections are damaged could help us predict what treatments are best for different research subjects and, eventually, might help us select the best treatment strategies for individual patients.

* See Abbreviations on p. xxvii.

Because the newer functional and structural neuroimaging techniques have enormous implications for rehabilitation research and development, it is highly desirable that rehabilitation researchers be able to evaluate the usefulness of the techniques for rehabilitation research and that the consumers of rehabilitation research (i.e., clinicians and researchers) be able to evaluate findings from research that has applied the techniques. The purpose of this article is to discuss functional and structural imaging techniques used in rehabilitation research. We will not cover routine clinical MR or X-ray computerized tomography images. Rather, we will concentrate on a variety of techniques used most frequently, though not necessarily exclusively, in research settings. The article will consist of two main sections:

1. A large number of MR techniques will be discussed, because of their extraordinary versatility.
2. Other functional neuroimaging techniques will be discussed, including positron emission tomography (PET), magnetoencephalography (MEG)/magnetic source imaging (MSI), near infrared spectroscopy (NIRS), transcranial magnetic stimulation (TMS), and electroencephalography (EEG)/evoked potentials. For each imaging modality, we will briefly explain the modality, discuss its uses and potential uses in rehabilitation research, discuss its strengths and limitations, and provide an example of research in the area.

FUNCTIONAL IMAGING

Functional MR imaging (fMRI) is but one form of functional imaging. Before we discuss fMRI or the other forms of functional imaging covered after the discussion of MR imaging (MRI) techniques, we must make several introductory comments about functional imaging. The working knowledge of functional imaging necessary to peruse the growing literature using functional imaging in rehabilitation requires familiarity with (1) the measures on which different kinds of functional imaging rely, (2) the goals of functional imaging, and (3) common methodological issues.

To begin, functional imaging attempts to measure neuronal activity. Some techniques measure neuronal activity relatively directly by measuring changes in electrical activity as clusters of neurons become active (i.e., EEG) or by measuring the changes in magnetic fields related to electrical activity changes (i.e., MEG).

While these techniques measure activity of neuronal clusters in real time, they do have limitations. One such limitation is that measuring changes in electrical activity/B_0 in deep brain structures is difficult.

When neurons become active, their need for energy drives changes in metabolism. Hence, another form of functional imaging measures these metabolic changes as a proxy for neuronal activity. Regional metabolic changes have been measured with PET by tagging fluorodeoxyglucose (FDG) with a positron emitting isotope (^{18}F) or by using a positron emitting isotope of oxygen (^{15}O). In practice, it takes a relatively long time (several minutes) to absorb enough labeled glucose to measure metabolic activity, and measuring oxygen metabolism has proven to be difficult.

Thus, many functional imaging techniques today do not rely on direct measures of metabolism. Rather, they rely on measures of hemodynamic responses. The increase in metabolic activity that supports regional increases in neuronal activity drives increases in blood flow to deliver the fuel for metabolic activity and carry away unneeded by-products of metabolism. One PET method frequently used to measure changes in blood flow is to tag water with a positron-emitting oxygen isotope ($H_2{}^{15}O$) and inject it intravenously. It takes at least 40 seconds to accumulate enough positron-emitting events and at least two scans under different conditions to measure changes in cerebral blood flow (CBF) between the conditions. Other ways to capture regional hemodynamic responses exist. For example, it has long been known that oxygenating blood changes its visible and infrared absorption spectrum. These changes can be measured near the surface of the brain with NIRS. When a brain region becomes active, the increase in blood flow overshoots the metabolic need of the tissue for oxygen, and even though oxygen consumption increases, a higher level of oxygenation exists in

blood, leaving the active region than exists in blood leaving the same region at rest. fMRI also relies on these changes in blood oxygenation to measure hemodynamic responses related to neuronal activity. For a relatively brief event of a second or two, the hemodynamic response takes about 12 to 15 seconds to evolve. While this is better temporal resolution than $H_2{}^{15}O$ PET, it is still relatively far from an instantaneous measure of neuronal activity.

We will cover each of the functional imaging techniques mentioned in greater detail later, with examples. We refer the reader wishing to read further about the history of functional brain imaging to a chapter by Raichle [1].

In general, functional imaging can be used in two ways. The first is to look at baseline levels of brain activity. In the early days of PET, ^{18}F-labelled FDG (^{18}FDG) was frequently used to measure baseline regional cerebral metabolism. For example, Metter et al. measured cerebral metabolism in patients with stroke and aphasia, and they defined regions outside the area of infarcts that showed decreased metabolism, which helped explain behavioral deficits [2]. More recently, MRI has been used to measure baseline cerebral perfusion. For example, Love et al. found they could explain the neural basis of reading deficits in a patient with left hemisphere lesion when, in addition to structural MRI, they used arterial spin labeling (ASL), an MRI technique that allowed them to image hypoperfusion in the left inferior parietal lobule [3]. This region did not show a lesion on standard structural images. While useful, such measures of baseline brain function do not define what brain areas are actually responsible for cognitive and behavioral activities. Over the past 20 years, functional imaging has been more commonly used to image regional changes in brain function that occur as a result of engaging in specific activities. Thus, the second way in which functional imaging has been used is to define regions that become active during specific behaviors and cognitive activities. At its simplest level, this form of imaging compares brain activity during contrasting states to define brain systems responsible for behavior. As examples, this form of functional imaging has been used to determine changes in motor cortex maps during rehabilitation [4] or to map changes in brain systems responsible for language during rehabilitation [5–6]. Most of our discussion on functional neuroimaging will cover this latter type of functional imaging, where brain regions responsible for specific behaviors are mapped.

As mentioned, mapping brain regions responsible for cognitive or behavioral functions involves comparing images from two or more states. A baseline or control image or state always exists from which changes can be defined. For example, to map areas of cortex responsible for moving a limb, images acquired during movement are compared with images during which no movement is made. On the surface, the idea of comparing two or more images to derive a map of regions responsible for a specific kind of behavior seems relatively simple. In practice, it can be quite complex. One strategy for doing so involves taking a complex cognitive task with several components and comparing it with a baseline or control task with all of the same elements except the one of interest. Peck et al. showed one of the potential problems in using this strategy [7]. In an fMRI experiment with neurologically normal subjects, they wished to isolate processes related to ordering the words in a sentence (i.e., syntax). They showed subjects a picture depicting a subject, an action performed by the subject, and a recipient of the action. The process of generating a sentence involved not only ordering the words in the sentence correctly but also retrieving the proper words for the items pictured. Picture naming could be used as the control task for sentence generation since it included all of the elements of the sentence generation task except for the ordering of words. However, when this was tried, Broca's area, which has been shown to be involved in syntax in both lesion and functional imaging studies, did not show any activity. This is probably because Broca's area is involved in word-finding processes as well as in syntax, although it could also be because these types of subtle difference comparisons result in changes in the blood oxygenation level dependent (BOLD) fMRI signal below the detection or noise threshold. Hence, when two cognitive tasks use the same neural component for different kinds of processing, it is not a good idea to use one as a baseline or control task for the other. When these investigators used passive viewing of

nonsense object pictures as a baseline task, activity in Broca's area was visible. In another study with neurologically normal subjects, Newman et al. demonstrated greater extent of activity in language eloquent cortex when phoneme discrimination was compared with a resting baseline than when the baseline task was either tone discrimination or passive listening to the same stimuli as used in phoneme discrimination [8]. Damage to the neural components of systems responsible for behavior, and especially cognitive functions like language, may produce unpredictable recruitment of undamaged structures to accomplish relevant tasks, even though such areas are not normally recruited. Hence, cognitively similar tasks are more likely to recruit overlapping areas in subjects with brain damage than in neurologically nondisabled subjects. This reasoning suggests that caution should be used regarding the use of cognitively similar processes as baseline and experimental tasks in individuals with brain damage. Hence, selection of simpler baseline tasks may useful in functional imaging studies of rehabilitation. For readers wishing to explore the issue of baseline tasks more completely, Petersen et al. have provided an excellent discussion of the matter [9].

Another important issue in studies of rehabilitation with populations with brain damage is mapping activity around lesions. An important issue in studies of aphasia is whether perilesional structures in the left hemisphere or structures in the previously nondominant right hemisphere are responsible for recovery of function or the effects of rehabilitation. This issue also has been addressed in studies of the motor system. In studies of subjects without well-demarcated areas of brain damage, the most frequently used analytic techniques involve deforming images of individual subjects into a common atlas space and averaging images across subjects to determine where significant activity differences between tasks or groups exist. A key assumption in this type of analysis is that tissue examined in any particular voxel for one subject corresponds to the tissue for that voxel in atlas space for any other subject in the sample (voxels are the basic three-dimensional volume units containing the quantitative data from which functional images are made). The problem with this assumption for patients with strokes (ischemic or hemorrhagic) is that the lesions vary considerably in shape, size, and location. The same voxel that is occupied by perilesional activity in one subject may be occupied by lesion in other subjects, and combining images across subjects may average away important perilesional activity. Thus, when examination of activity in the lesioned hemisphere is important, another data analysis approach must be used.

These are but a few examples of the complexities in functional neuroimaging research. In addition to these more general challenges, each functional imaging technique has its limitations and problems, some of which we will discuss in the following sections. However, it is difficult in this survey of functional neuroimaging to cover all the difficulties that arise in research, or indeed in clinical applications. Instead, we will endeavor to cover the most commonly encountered problems with each technique.

MAGNETIC RESONANCE IMAGING AND SPECTROSCOPY

Basic Principles

Since a number of the techniques for brain imaging discussed in this article rely on MR technology, it is worth some space to describe a few basic principles of MR imaging and spectroscopy. Nuclei of atoms comprise protons and neutrons. Isotopes that have an odd number of either protons or neutrons have a nonzero spin and an associated nuclear magnetic moment (i.e., nuclear magnetism of specific strength and direction); those with an even number of both protons and neutrons have no magnetic moment and are not observable with nuclear magnetic resonance (NMR, often shortened to MR).

Nuclear magnets can align parallel or antiparallel to the applied DC magnetic field (B_0). Since slightly more align with the field than against, a net macroscopic nuclear magnetization (M) exists. As a result of the property of spin, nuclear magnets have angular momentum causing them to precess around an applied B_0. Precession can be thought of as a wobbling of the magnetic moment around the B_0, similar to the way a toy top both spins and precesses

about its gravitational vector. The frequency of precession in B_0 of a specific strength is called the Larmor frequency. The direction of precession depends on the parallel or antiparallel orientation of the magnetic moment about the B_0 axis, with precession occurring in opposite directions for the parallel versus antiparallel orientations.

If a radiofrequency (rf) field with the Larmor frequency (rf pulse) is briefly applied to the sample, the spins can absorb energy and flip between the energy state levels. This moves the vector M out of alignment with B_0, and it precesses around B_0 and creates an oscillating magnetic field that can be detected with a coil in which a sinusoidal voltage is induced. The degree to which the vector M tips out of alignment with B_0 (i.e., the flip angle) depends on the strength and duration of the rf pulse. The signal induced in the rf coil decays with a time constant referred to as T_2. T_1 is a time constant that describes the time it takes M to return, or relax, to its original state of alignment with B_0. In biological samples, T_2 is shorter than T_1. By varying image acquisition parameters, one can produce T_1-weighted images (where cerebrospinal fluid has low signal relative to gray and white matter) or T_2-weighted images (where cerebrospinal fluid has high signal relative to gray and white matter). Other types of weighting are possible.

In general, many rf excitation pulses must be used in data acquisitions, and the time between excitation pulses for a given slice of tissue is referred to as the repetition time (TR). In fMRI, the TR determines how quickly a single brain image is acquired. To analyze how signal changes in concert with experimental manipulations, it is necessary to acquire many brain images during an fMRI experiment. The time from application of the rf excitation pulse to the signal acquisition is referred to as the echo time (TE). In BOLD fMRI (see later explanation), the most common form of fMRI, a relatively long TE will yield greater changes in functional signal between activation and baseline states, but will also cause greater artifacts near air-tissue interfaces and lessened overall signal intensity. Hence, the choice of a TE in BOLD fMRI will often be a trade-off between the need to produce a relatively strong signal and the desire to limit artifacts.

Water, the most ubiquitous hydrogen-containing molecule in the body, offers a medium for MRI and resonates at a single frequency in a uniform B_0. However, the Larmor frequency and phase of precession can be manipulated by creating slight gradients within the main B_0, such that the strength of the field varies with a linear relationship to distance. Within an acquisition plane (image slice), the location of a signal in one direction is determined by slight changes in frequency and in the orthogonal direction by changes in phase of the induced signal. The third spatial dimension of the image is addressed by acquiring multiple relatively thin slices. Slice selection is also accomplished by creating a gradient in the B_0. All these gradients in the B_0 are created with gradient coils separate from the superconducting coil used to generate the B_0.

MR spectroscopy (MRS) can be used to detect some molecules in the brain other than water. Atomic nuclei in molecules have electrons associated with them in certain specific geometric spatial locations dictated by bonding forces to neighboring atoms. These orbitals constitute effective circuits through which the electrons circulate. In an applied B_0, these circulating currents induce a field in opposition to B_0, which shields the nucleus from the applied B_0. This means that, for example, hydrogen atoms in different parts of a molecule have different frequencies, or chemical shifts. Signals can be localized to voxels with use of selective excitation for single voxel spectroscopy or chemical shift imaging (CSI).

The physics of MRI and MRS is much more complex than can be described in the available space. We have endeavored to provide the reader with a brief description of some of the more common concepts. We refer the reader wishing greater detail to the excellent text by Buxton [10].

Functional Magnetic Resonance Imaging

BOLD-Contrast fMRI

At the time of this article, BOLD contrast is the most common method for obtaining fMRI.

BOLD contrast is derived primarily from the paramagnetic properties of deoxygenated hemoglobin (deoxyhemoglobin). Paramagnetic materials tend to concentrate magnetic flux, decreasing the MR signal when a pulse sequence sensitive to magnetic susceptibility differences is used. Hence, regional cerebral increases in deoxyhemoglobin will cause decreases in the MR signal for the region. However, the underlying phenomena generating BOLD contrast are not as straight-forward as it might seem at first glance. When an area of the brain becomes active, metabolism increases to support the activity. Aerobic metabolism increases oxygen extraction, and concentrations of deoxyhemoglobin transiently increase in active areas, thereby decreasing MR signal. However, regional CBF (rCBF) then increases to deliver more oxygenated hemoglobin for the increased local metabolism. The increase in rCBF exceeds what is needed to supply the active tissue with oxygen; therefore, the relative concentration of deoxyhemoglobin per unit volume in the active region decreases, peaking the BOLD signal roughly 6 seconds later due to this overcompensation in perfusion. Thus, the BOLD signal is the result of a complex interplay between changes in regional cerebral oxygen extraction, blood flow, and blood volume. A hemodynamic response triggered by an event taking 1 second to occur generates a hemodynamic response that typically shows an increase in signal lasting 10 to 12 seconds to rise to peak and return to baseline. This positive change in signal may be followed by a negative phase of several seconds, but this phase is often considered of no interest. **Figure 1** shows an example of a hemodynamic response derived from our research. The *x*-axis represents time, and the *y*-axis represents percent of change in MR signal. We cover other types of fMRI later. We refer the reader to Buxton for a more detailed explanation of BOLD contrast [10].

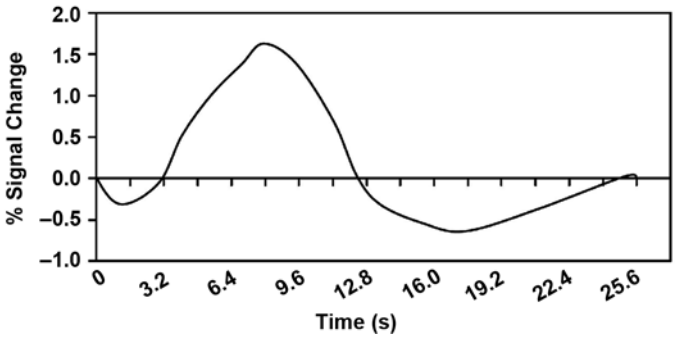

Figure 1.
Hemodynamic response expressed as percent change of total signal. Note that positive phase of response takes around 12 seconds to resolve.

fMRI has specific advantages and disadvantages relative to other functional neuroimaging techniques. One advantage of BOLD-contrast fMRI over PET, another form of functional imaging, is that BOLD-contrast fMRI is noninvasive and does not expose the subject to radiation. The contrast in this form of fMRI is endogenous, i.e., BOLD contrast takes advantage of existing substances in the body to produce images. PET images require the injection of a radioactive, positron-emitting contrast agent. Another advantage of fMRI over other imaging techniques is its spatial resolution. Spatial resolution refers to the degree of accuracy with which brain activity (i.e., hemodynamic responses) can be located in space. The spatial resolution of fMRI is limited by the voxel size in which images are acquired. The voxel size in fMRI images in human studies is most often driven by practical, as opposed to physical, considerations. Specifically, a trade-off exists between spatial and temporal resolution. Acquiring data in smaller voxels takes more time than acquiring data in larger voxels because it takes more small than large voxels to cover the brain. Practically speaking, $2 \times 2 \times 2$ mm voxels are the lower limit of what it is practical to acquire in whole-brain fMRI images on a conventional 1.5–3 T scanner. However, acquiring smaller voxels than that is possible, especially if whole-brain images are not needed or stronger magnets are available. Temporal resolution refers to the degree of accuracy on a temporal scale with which a functional imaging technique can describe when a neural event occurred. Temporal resolution is an advantage for fMRI over PET, but fMRI is at a disadvantage in temporal resolution compared with techniques using EEG or MEG. PET's ability to resolve neural events is on the order of tens of seconds, fMRI's ability to do so is on the order of seconds, and the ability of EEG- and MEG-based techniques to do so is on the order of milliseconds. Since the cascade of events through neural systems

happens on the millisecond scale, EEG- and MEG-based techniques are most likely to be useful when this kind of temporal information is needed. PET and fMRI can both image activity in deep subcortical structures, whereas this is difficult, if not impossible, with EEG- and MEG-based techniques. Another advantage of fMRI is the ubiquity of MRI scanners, and most have the potential to be used for fMRI. By comparison, PET scanners are not as common, and to use PET as a functional imaging technique for cognitive processes, it is necessary to have a cyclotron and a radiochemist nearby. Another advantage for fMRI is that the same platform used to acquire functional images can be used to acquire high-resolution anatomic images in the same space as functional images, so that functional images can be overlaid onto structural images to allow for precise anatomic localization. PET, MEG, EEG, TMS, and NIRS all have to rely on structural MR images and/or atlases to localize activity in the brain. Cost can be a disadvantage for fMRI if there is not a readily available instrument to acquire images. Relative to EEG-based techniques, fMRI is expensive. MRI scanners cost millions of dollars, and their maintenance can be expensive as well. However, PET and MEG-based techniques have similar costs for implementation. Other disadvantages of fMRI include the confined space in which participants must be placed, which can induce claustrophobia in susceptible participants, and the acoustic noise required to obtain scans, to which the brain inevitably reacts.

The use of fMRI in rehabilitation studies is just beginning. In locomotor rehabilitation, early evidence suggests that the amount of cortex involved in a related motor function (ankle dorsiflexion) expands as a 12-week rehabilitation program approaches its midpoint and then contracts again toward the end of treatment. It also appears that representations for the lower limb can expand into cortex adjacent to their normal location [4]. Findings in the aphasia rehabilitation literature are less clear, and a controversy exists regarding whether the right or left hemisphere is the site of rehabilitation gain in premorbidly right-handed patients. A review of the literature suggests that both the right and left hemispheres may contribute under different circumstances, or indeed, within a single patient. The contribution of the left hemisphere may be greater in small lesions, while the contribution of the right hemisphere to treatment gains may be greater in large lesions [11]. A number of technical obstacles must be overcome to use fMRI in aphasia treatment studies, particularly if language production is the target of treatment. We refer the reader interested in more details to the review by Crosson et al. [11].

Eventually, fMRI might be used to predict what treatment will work with which patient, to determine what structures can be recruited for rehabilitation, and/or to measure brain system changes that result from rehabilitation. However, a good deal of research must be accomplished before we reach that point.

The following is an example of using fMRI in rehabilitation research from our own laboratory [12]. In 2007, we demonstrated that a treatment designed to relateralize language-production mechanisms from the left to the right frontal lobe produced a faster rate of relearning of words than a similar control treatment [13]. The treatment used an intention manipulation (complex movement of the left hand to initiate naming trials) because we thought that this manipulation would help to relateralize language production mechanisms. To assess whether or not the treatment actually relateralized frontal activity to the right hemisphere, we administered a category-member generation task to five patients during fMRI before and after the intention treatment. Four of the five patients improved during treatment. The four patients who improved in treatment showed a significant rightward shift in lateral frontal activity, which became more concentrated in the ventral portion of the right motor/premotor cortex or in pars opercularis just anterior to motor/premotor cortex. Although laterality of frontal activity for those four patients was not different from that of controls before treatment, frontal activity was significantly more lateralized to the right hemisphere than in controls after treatment. With the exception of the right hemisphere in one patient, activity in both frontal lobes decreased from pre- to posttreatment fMRI, suggesting greater efficiency of processing after treatment. The one patient who did not improve in treatment showed a leftward as opposed to rightward shift in lateral frontal activity and an increase in left frontal activity. **Figure 2** shows the pre- and

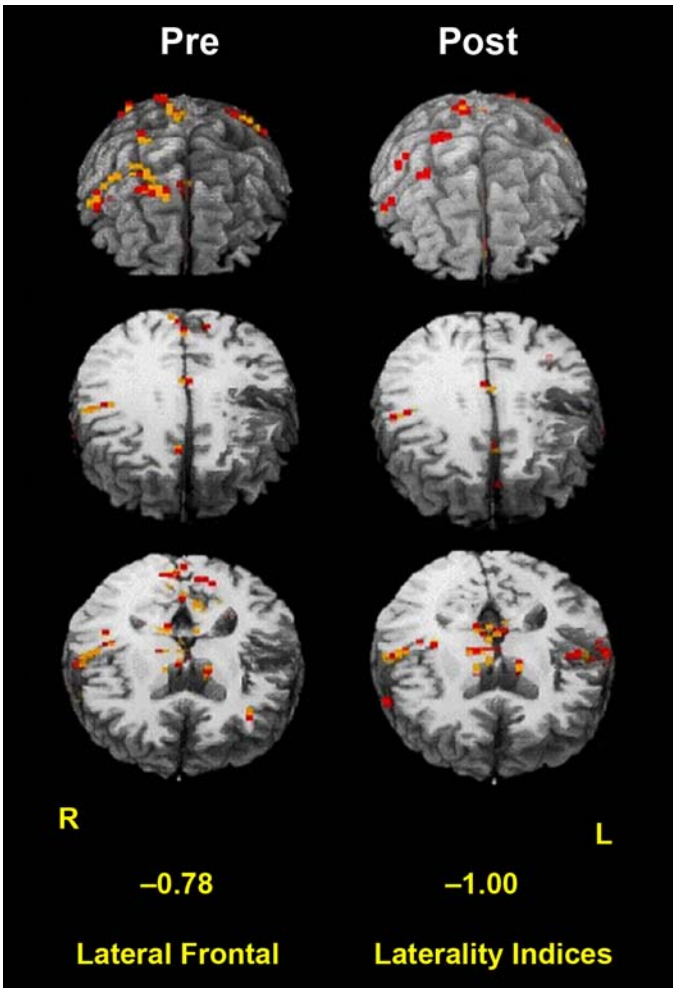

Figure 2.
Pre- and posttreatment images for one subject who received intention treatment. Red represents $R^2 > 0.20$; orange represents $R^2 > 0.25$. Note lack of left frontal activity on post- compared with pretreatment images, and general reduction in frontal activity from pre- to posttreatment. Lateral frontal laterality indices are displayed at bottom of image, with 1.00 representing activity entirely lateralized to left (L) and –1.00 representing activity entirely lateralized to right (R).

posttreatment activity most typical of those patients who improved in treatment. The images have been equated for sensitivity to BOLD responses between the two sessions. Note the total lack of left frontal activity in post- compared with pretreatment images, indicating a rightward shift in lateral frontal laterality, and the reduction in activity in the right as well as the left frontal lobe, suggesting greater efficiency of processing post- compared with pretreatment. This study is of interest because it indicates that it may be possible to target specific brain structures for rehabilitation and use functional imaging to confirm the success of the strategy. The ability to perform this kind of study eventually should lead to development of better treatments for aphasia.

Other Forms of fMRI

While BOLD contrast is by far the most common form of fMRI, other kinds of fMRI exist. The reasons that these forms of imaging have not gained as widespread usage and acceptance as BOLD-contrast fMRI are variable. We will briefly discuss these reasons and describe the following three techniques: ASL, blood oxygenation sensitive steady-state (BOSS), and dynamic susceptibility contrast (DSC). In addition, we will describe resting state or functional-connectivity MRI (fcMRI), which is fMRI without a specific task and provides a passive means of interrogating functional brain networks and their connectivity.

ASL measures CBF using an endogenous tracer, blood water, to noninvasively measure tissue perfusion to evaluate the tissue viability or functionality [14–15]. In ASL, two sets of images are alternately acquired: a set of labeling images and a set of control images (**Figure 3**). In the labeling experiment, arterial blood spins on the proximal side of the imaging slab are inverted. After a short delay of a second or so to allow arterial blood that is tagged in this fashion to perfuse throughout the brain, images are acquired from the imaging slab. In the control imaging experiment, no arterial blood is inverted, and after the same short delay, images are acquired from the imaging slab. After pairwise subtraction of control from labeling images, MRI signals from static brain tissue can be cancelled, leaving signal only from the labeled inflowing blood water perfusing brain tissue. The difference image from pairwise subtraction of control images from labeling images is referred to as a perfusion-weighted image. With an appropriate perfusion model, CBF maps can be reconstructed [16]. Several variants of ASL techniques exist [15].

The application of inversion rf pulses can generate magnetization transfer (MT) effects on tissue [17]. In MT, irradiation of broad signals from macromolecules to which water is transiently binding changes

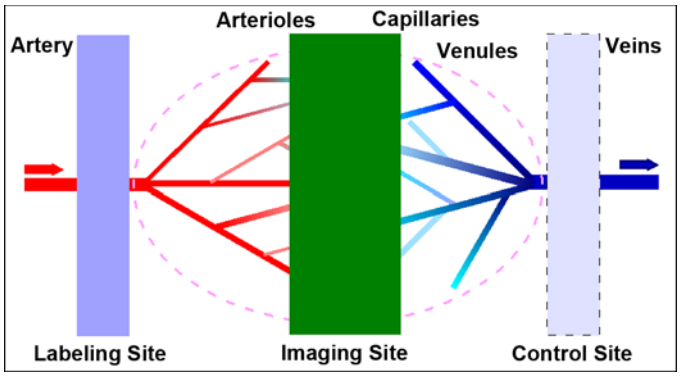

Figure 3.
Schematic diagram for arterial spin labeling (ASL) imaging. Labeling of arterial blood is proximal to tissue of interest, as shown by blue plane at left. After delay to let labeled blood arrive at tissue sites, imaging acquisitions will be performed. In some ASL techniques, control experiments will be done using a symmetric labeling radiofrequency pulse at a distal site to minimize magnetization transfer effects (light blue plane at right).

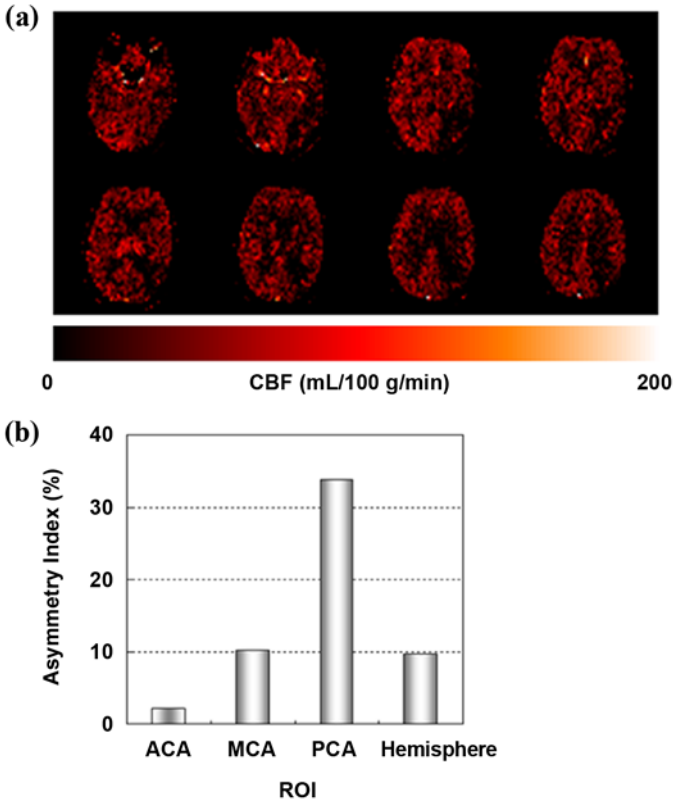

Figure 4.
(a) Cerebral blood flow (CBF) maps and **(b)** asymmetry analysis results from arterial spin labeling perfusion study of 76-year-old female patient with stroke. Asymmetry index (%) = [CBF(right) – CBF(left)]/[CBF(right) + CBF(left)] × 100. Specific perfusion territories are designated by anterior cerebral arteries (ACA), middle cerebral arteries (MCA), and posterior cerebral arteries (PCA). In **(a)**, brighter colors indicate greater CBF. Note decreased CBF in the posterior right side of images, consistent with greater asymmetry in CBF for the PCA distribution than ACA and MCA. In **(b)**, the negative index value for ACA is indicated with different bar pattern. ROI = region of interest.

the water signal intensity. If the MT effects are not the same between the labeling and control experiments, these MT effects can confound ASL perfusion signals. Using either an asymmetric control rf pulse in the same proximal site or a symmetric control rf pulse in the mirrored distal site can control MT effects by using the same rf pulses as in the labeling experiment, with adjusted radiation frequency.

ASL has become particularly useful in circumstances where baseline CBF measures are useful. For example, ASL showed a hypoperfused area in the left parietal cortex of a patient with stroke, consistent with the patient's reading deficit, which appeared normal on conventional anatomic images [3]. **Figure 4** shows an example of this type of application of ASL from one of our own laboratories. Measuring quantitative CBF changes induced by pharmaceutical agent challenge is also promising for clinical application of ASL. For example, the specificity of cerebral perfusion changes under hypercapnia or hypocapnia states has been evaluated [18]. The effects on CBF of other drugs that can alter the physiological or neurophysiologic states of the brain have also been studied by ASL. For example, the global increase of brain perfusion with remifentanil challenge is mainly due to remifentanil's depression of breathing and the consequent increase of blood $PaCO_2$ [19]. In another ASL perfusion study, acetazolamide, a carbonic anhydrase inhibitor, was administrated to evaluate the augmentation of CBF with patients with ischemic symptoms due to arterial stenosis [20].

ASL also can be used for functional images, although fMRI has not become a widespread use for ASL. One problem with most ASL techniques is that it is hard to acquire whole-brain fMRI on a time scale that would allow for visualization of the hemodynamic response. Hence, the investigator has to be satisfied with a few image slices covering critical areas. However, in ASL fMRI, a much shorter TE is usually used than in BOLD fMRI, which reduces the signal

loss due to susceptibility effects and provides better spatial specificity than BOLD MRI, where large draining veins can contribute artifactual signal. For example, Kemeny et al. demonstrated that ASL could be used to collect fMRI data during sentence production in such a way as to eliminate artifacts present on BOLD images when subjects speak [21]. We refer readers desiring more detail on ASL to this article on techniques [15] and the companion article on applications [22].

BOSS relies on a change in the MR signal frequency for deoxyhemoglobin relative to oxyhemoglobin. The BOSS acquisition capitalizes on this signal shift to collect images in which the signal from oxyhemoglobin will be positive and the signal from deoxyhemoglobin will be negative. BOLD and BOSS fMRI both measure signal changes resulting from the deoxyhemoglobin frequency shift. However, BOLD-contrast fMRI measures that frequency shift indirectly as signal dephasing and BOSS measures the shift directly. Because increased activity causes a drop in the proportion of negative deoxyhemoglobin-related signal and an increase in the proportion of positive oxyhemoglobin-related signal, the net BOSS signal increases during activity [23]. BOSS has advantages over BOLD. For example, BOSS has a higher signal-to-noise ratio than BOLD, with BOSS signal changes being roughly 2 to 3 times larger than BOLD. Further, BOSS is not subject to the signal dropout around air-tissue interfaces that plagues BOLD imaging. Among the reasons that BOSS fMRI has not become more popular are that it has not found its way into the commercially available sequences on MR instruments and that its implementation can be complex. We refer readers wishing more detailed treatment of BOSS to the work of Miller et al. [23–25].

DSC uses the paramagnetic property of gadolinium ions as a magnetic tracer. Gadolinium ions cause a transient disruption of the B_0 around the vessels through which it flows, resulting in a transient signal loss proportional to the amount of gadolinium. The signal loss can be used to determine changes in relative cerebral blood volume at the voxel level. Advantages to this technique include its high contrast-to-noise ratio, which can be used to overcome artifacts during patient speech. The major drawback to DSC is its invasiveness, since intravenous injection of gadolinium complexes is necessary. Naeser et al. used DSC to study brain activity during narrative language in patients with chronic nonfluent aphasia [26]. These authors also briefly describe the technique.

fcMRI detects interconnected brain regions which activate together as a functional network. It is most often performed as resting-state fMRI without a specific task, in which the brain pseudorandomly activates under little or no guiding external influence. Since no task performance is required on the part of the subject, the resting state implementation has the advantage of being a passive method of interrogating functional brain networks and their functional connectivity. This is an obvious benefit for application to stroke and other pathologies that can make task performance and monitoring difficult.

The acquisitions for fcMRI should have about 300 volumes or serial time points to adequately sample the low-frequency signal fluctuations (<0.1 Hz) representative of vascular fcMRI responses to baseline neuronal activity "at rest." Collecting cardiac and respiratory waveforms in conjunction with the fcMRI time course data is useful for regressing out signal fluctuations due to these nonneuronal sources of physiological variability, leaving signal fluctuations more nearly caused by vascular responses to neuronal activity [27]. Calibration of the BOLD effect using breath hold [28] or amplitude of resting state signal fluctuations [29] reduces variability of individual vascular reactivity and improves group averages and comparisons.

Analyses of fcMRI data are typically done in one of two ways: unguided exploratory analyses by Independent Components Analysis [30], or seed-based analysis by which voxels whose signal time course correlates highly with those of the seed region of interest (ROI) are detected [31].

Few examples exist in the literature of how fcMRI can be applied to stroke and rehabilitation. A left hemorrhagic posterior cerebral artery stroke produced increased functional connectivity between areas V4/V8 and V5 of the left hemisphere in comparison with the same areas in the intact hemisphere when the

subject viewed changing colors, suggesting that visual perception after the V1 lesion is mediated by subcortical pathways that bypass V1 and project first to V5 and V4/V8 and subsequently to V2/V3 [32]. Spatial neglect in subjects with stroke was studied by fcMRI in both acute and chronic recovery stages in dorsal and ventral frontoparietal areas [33]. Part of the lesioned ventral network was diffusely disrupted and showed no recovery, whereas in the structurally intact dorsal network, posterior parietal cortex connectivity was acutely disrupted but fully recovered. Disrupted connectivity in the ventral network correlated with impaired attentional processing and disconnection of the frontal and parietal cortices was associated with more severe spatial neglect. A recent review highlights studies that have combined structural (DTI, see "Diffusion Imaging and Diffusion Tensor Imaging" section) and functional (fcMRI) connectivity methods [34]. Information about brain networks and functional connectivity affected by stroke and rehabilitation can also be obtained from EEG [35–36] and MEG [32].

One weakness in fcMRI is the certainty with which inferences can be made regarding functional networks for specific cognitive or behavioral functions when acquisitions are made in the resting state. Recently, techniques to address functional networks during performance of relevant tasks have been developed. These include adaptation of structural equation modeling (SEM) and dynamic causal modeling (DCM) to define relationships between components of functional networks. A potential drawback is that these techniques work best when investigators have a model to test. Abutalebi et al. used DCM and fMRI to study recovery of functional connectivity in a bilingual patient who received therapy in his second language (L_2) but not in his first language (L_1) [37]. The functional connectivity of selected left-hemisphere language and cognitive control mechanisms increased across the course of therapy for L_2, consistent with increasing activity and language skills in these areas for L_2, while the functional connectivity of these structures decreased for L_1, consistent with stable to decreasing performance in L_1. Before therapy, functional connections were generally stronger for L_1 than L_2, but the reverse was true after therapy. We expect that DCM and SEM will be increasingly applied to rehabilitation.

Diffusion Imaging and Diffusion Tensor Imaging

Although fMRI has become a valuable tool for imaging changes in brain function as a result of rehabilitation, this versatile technology has also provided us with new methods of imaging brain structures, in particular the brain's white matter. Diffusion-weighted MRI (DW-MRI) is a noninvasive imaging technique that allows one to assess the structural integrity of tissues in vivo. DW-MRI measures the diffusion of water molecules, random motion present due to thermal energy. In tissues, diffusion is restricted by cell membranes as well as tissue boundaries, resulting in diffusion anisotropy, or diffusion along one preferred direction. For example, in white matter fiber bundles, the myelin sheath surrounding axons prevents diffusion across the axon, but not along the longitudinal axis of the axon. Therefore, the directionality of diffusion provides us with information about local fiber orientation.

Mathematically, diffusion in a given voxel can be characterized by an ellipsoid, or tensor, oriented along the direction of the fiber [38]. The major axes of the ellipsoid, called eigenvectors, describe spatial orientation of the fibers. The lengths of the axes, known as the eigenvalues, describe the strength of diffusion along each of the three axes. The diffusion of water in white matter fiber bundles would be described by an ellipsoid elongated along the principle diffusion direction (PDD), or the longitudinal direction of the fiber. A scalar describing the proportion of the diffusion along a particular direction (relative to all other directions) is called fractional anisotropy (FA). Values of FA range from 0 to 1, where 0 describes diffusion that is completely isotropic, or equal in all directions. For instance, isotropic diffusion is usually observed in the ventricles, because water molecules in CSF are able to disperse freely in all directions, described by FA values close to 0. White matter fiber bundles would exhibit FA values close to 1 because almost all diffusion is directed along the length of the axons. The average rate of diffusion, or mean diffusivity (MD), is another important scalar describing the average speed with which the molecules traveled during a

given time interval. MD values are higher in the ventricles, because molecules are unrestricted and can travel larger distances than in gray or white matter. Together, FA and MD maps can be used in clinical settings to acquire information about the structural organization of tissues not present in conventional MRI. For example, the sensitivities of FA and MD measures have been shown to reveal damage in white matter in ischemic leukoaraiosis abnormalities not noticeable on T_2-weighted MR scans and to reveal Wallerian degeneration poststroke months before it could be detected by T_1-weighted MRI [39–40]. Group studies investigating white-matter abnormalities have used FA measures to localize differences in the white matter in patients with primary lateral sclerosis, amyotrophic lateral sclerosis (ALS), and multiple sclerosis (MS), as well as to correlate these differences with the Expanded Disability Status Scale [41–42]. In nondisabled populations, FA measures were shown to reflect effects of myelination correlated with hours of practice in professional piano players [43].

Generally, FA and MD values are negatively correlated with higher MD values and lower FA values, indicating underlying tissue degeneration. However, an inverse relation between these measures is not always observed. Lower FA values indicate a reduction in preferred directionality of diffusion. However, decreased fiber integrity in secondary directions can artificially drive the FA value closer to 1 while MD is also increasing [44]. In such cases, the FA value would not be a good indication of white-matter integrity. Thus, to better describe structural changes in white matter in neurological disease, it is important to consider whether multiple DW-MRI measures provide converging evidence. **Figure 5** shows images based on MD (**Figure 5(a)**), FA (**Figure 5(b)**), color coded PDD maps from FA (**Figure 5(c)**), and fiber tracts derived from DTI data (**Figure 5(d)**).

In addition to assessment of white-matter integrity, DW-MRI also allows for white-matter visualization using tractography. Tractography approaches that trace the fibers by following the PDD are called streamline. Although streamline methods produce robust results for large white matter tracts, such as the corticospinal tract (CST), they have difficulty

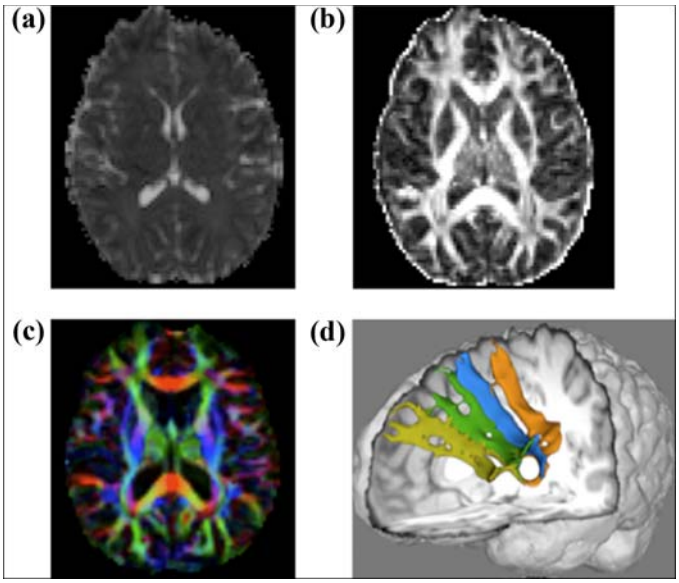

Figure 5.
Diffusion-weighted magnetic resonance measures. **(a)** Mean diffusivity map, **(b)** fractional anisotropy (FA) map, **(c)** FA map overlaid with principle diffusion direction in color (red left to right, blue inferior to superior, green anterior to posterior), **(d)** three-dimensional rendering of previously undocumented fiber paths connecting Broca's area (Brodmann's areas 44/45) with supplementary motor area (SMA) (orange), pre-SMA (blue), Brodmann's area 8 (dark green), and Brodmann's area 9 (light green).

accurately representing branching or crossing fibers, since in this case no single principal direction exists. A second category, called probabilistic tractography, should be used to properly represent fiber architecture. Probabilistic tractography approaches trace the tracts in many possible directions, recording probabilities associated with each direction. Thus, at the intersection of two tracts, both fibers will have comparable probabilities associated with each corresponding direction, each of which will be traced by the algorithm. In stroke rehabilitation studies, ratios computed as the ipsi- over contralesional hemisphere tract volumes (numbers of voxels) were shown to correlate with recovery [45]. In patients with ALS, progression rates have been correlated with DW-MRI measures of structural integrity in the CST fibers, using connectivity measures generated by a probabilistic tractography approach [46].

In summary, DW-MRI provides clinicians with many useful tools sensitive to changes in the white

matter. Moreover, these tools provide researchers with information, such as fiber tract visualization, that has previously been available only in primate studies and cadaver dissections. DW-MRI allows us not only to investigate changes in structural organization of known white matter projections but also to ascertain the presence of new pathways, making it crucial to understanding mechanisms of neurological disease. For example, **Figure 5(d)** shows the visualization of fibers between medial frontal cortices and Broca's area,* both of which are involved in word production. One potential use of DW-MRI in rehabilitation involves the measurement of integrity of various tracts and correlating these measures with behavioral and cognitive measures or with measures of rehabilitation outcome.

Magnetic Resonance Spectroscopy

MRS provides a noninvasive way of investigating brain chemistry. Although MRS can be performed using a number of different nuclei, we will only describe the most clinically established method, ^{1}H spectroscopy. With it, important brain metabolites such as N-acetylaspartate (NAA), creatine (Cr), and choline (Cho) can be measured, as well as molecules with weaker signals such as glutamate, glutamine, myo-inositol, and lactate (Lac) [47]. Resonances (peaks) are identified by their position (chemical shift) in the spectra, expressed in parts per million (ppm) relative to a standard frequency. Peak areas are related to the metabolite concentrations. The dominant peaks are from the acetyl group of NAA at 2.0 ppm, total Cr at 3.0 ppm, and total Cho at 3.2 ppm (**Figure 6**).

NAA is an amino acid present mostly in neurons and is widely regarded as a marker of neuronal structural and functional health and integrity. Decrease of NAA is observed in various cerebral pathologies such as ischemia, brain tumors, gliosis, dementia, trauma, and MS. It is rarely increased, one exception being Canavan's disease. Longitudinal MRS studies in patients with stroke have found acute decreases in NAA and a continuing fall during the first week after the onset [48–49]. Recovery of the NAA levels has been observed in certain cases of reversible ischemia [50] and acute brain injury [51], making NAA an important clinical outcome marker, as reviewed recently [52]. Effects of rehabilitation and interventions have also been studied, indicating relations between metabolite changes and brain reorganization and plasticity [53]. NAA significance and changes under various conditions has been reviewed [54].

The total Cr (Cr and phosphocreatine) peak is a marker of the energetic status of cells and is often used as a standard or reference for relative quantification of other metabolites due to its relative consistency with location in the brain, age, and physiological conditions. However, caution needs to be exercised, since Cr levels do change in certain pathologies such as tumors and stroke.

The total Cho peak (phosphocholine, free Cho, and glycerophosphocholine) is a marker of cell membrane integrity and viability. It has been shown to be elevated in dementia, MS, aging, and tumors [55].

Lac is below the MRS detection threshold in a nondisabled brain but is measurable in ischemia and hypoxia, since it is the end product of anaerobic processes [56].

Both data acquisition and analysis in MRS usually require significant technical expertise. In single voxel spectroscopy, a proper and reliable localization of the volume of interest is important and usually requires an MR operator with a good knowledge of brain anatomy. The quality of the acquired spectra (the line width and spectral resolution) depends on the homogeneity (shimming) of the of B_0. Most of the MR vendors provide autoshim utilities, but in some brain areas, a manual adjustment of the shim currents is often necessary. The water signal is orders of magnitude higher than the metabolite signal, so efficient water suppression is important as well. In CSI techniques, extra effort needs to be taken for lipid signal suppression.

Processing the MRS data is, in general, complicated because of overlapping peaks and the limited signal-to-noise ratio of in vivo spectra; accurate quantification requires close attention to a number of details [57]. An automatic postprocessing tool that has gained popularity in both clinical and research

* Ford, Anastasia. Unpublished data. 2010.

settings is the Linear Combination Model, which uses prior spectral knowledge by analyzing the in vivo spectrum as a linear combination of in vitro acquired metabolite model spectra (vendor provided or locally acquired) [58]. Simulated lipid and macromolecule signals are also included in the modeling. Accurate accounting for these signals is crucial for proper metabolite quantification, especially at short TE, which provide inherently higher signal-to-noise ratio.

Absolute metabolite quantification [59–60] requires internal [61] or external [59–60] reference standards. A number of instrument-dependent factors, as well as in vivo relaxation corrections, complicate the quantification procedure. Since relaxation corrections are usually difficult to measure in vivo because of time constraints, it is often recommended to use sufficiently long TR and as short as possible TE in the data acquisition [61–62].

Despite technical challenges, MRS is a valuable tool for measuring biochemical changes in the brain in various pathologies and in recovery and rehabilitation.

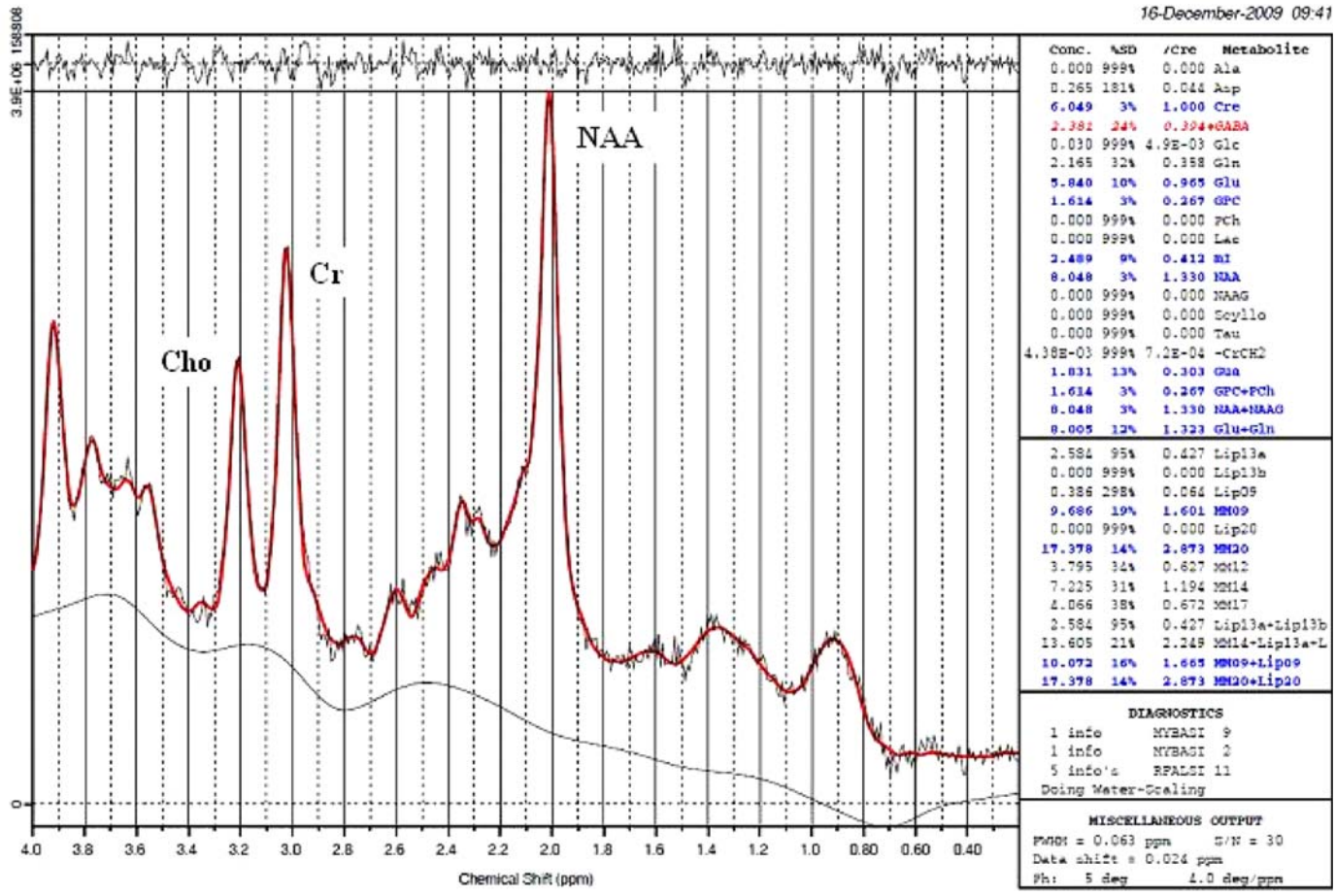

Figure 6.
An example ^{1}H spectrum, acquired at 3 T, of left basal ganglia of nondisabled control subject, postprocessed in Linear Combination Model [1–2]. Metabolites included in modeled basis spectra are shown in table on right. Those detected with reasonable confidence are in blue. Percent standard deviation (%SD) indicate Cramer-Rao lower error bounds. Cho = choline, Cr = creatine, NAA = N-acetylaspartate, ppm = parts per million.

1. Provencher SW. Estimation of metabolite concentrations from localized in vivo proton NMR spectra. Magn Reson Med. 1993;30(6):672–79. [PMID: 8139448]
DOI:10.1002/mrm.1910300604
2. Provencher SW. Automatic quantitation of localized in vivo 1H spectra with LCModel. NMR Biomed. 2001;14(4):260–64. [PMID: 11410943]
DOI:10.1002/nbm.698

OTHER FUNCTIONAL NEUROIMAGING TECHNIQUES

Positron Emission Tomography

Although today fMRI is the dominant form of functional neuroimaging for cognition, the field owes much to scientists who used PET as a tool for imaging cognitive systems before fMRI was a widespread technology. The technique relies on unique properties of short half-life positron emitting radionuclides to map brain systems responsible for cognition. Specifically, a positron is a particle that has the same mass as an electron but differs from an electron in that its charge is positive, not negative. When emitted from the radionuclide, a positron will travel a very short distance before encountering an electron with which it undergoes annihilation. As a result of this process, two 511-KeV photons leave the site of annihilation traveling almost exactly 180° from one another. PET images rely on rings of coincidence detectors and the concept that if two photons are detected coincidentally, it is highly likely that an annihilation event occurred on a straight line between the two points of detection. If enough of the events are detected, then a computer can be used to create images of the distribution of the radionuclide within the sample. ^{18}FDG was administered in many early PET studies to map baseline levels of regional glucose metabolism in the brain. ^{18}F has a half-life of 110 minutes. Typically, 30 minutes or more was allowed for nonmetabolized ^{18}FDG to clear the brain. With the remaining portion trapped in brain tissue, its distribution could be used as a good indicator of regional glucose metabolism levels. However, the 30 minutes needed to get a single image was not well suited to measuring changes in brain activity related to changes in cognition. Fortunately, increases in metabolism that occur with neuronal activity also drive increases in blood flow. A technique of injecting ^{15}O-labeled water ($H_2{}^{15}O$) into the bloodstream allowed PET investigators to image changes in rCBF due to cognitive activities performed during the roughly 40-second image acquisition. The relatively short half-life of ^{15}O (123 seconds) allowed for multiple administrations of the radionuclide, and images of cognitive activity could be compiled by assessing differences in rCBF between images collected during two different cognitive states. For more information on PET technology and its history, the interested reader may wish to consult the chapter by Raichle [1].

While $H_2{}^{15}O$-PET was better suited to measuring brain activity due to cognitive states than ^{18}FDG-PET, the former technique still has important limitations. One drawback to the technique is the exposure of subjects to radiation and the limited number of scans that this implies. From a practical standpoint, the most commonly used PET technique for exploring the brain's cognitive systems, measurement of rCBF changes using $H_2{}^{15}O$, is performed with a 123-second half-life contrast agent, which requires collocation with a cyclotron and a radiochemist. These requirements historically limited the availability of PET, whereas MRI scanners are much more common. Another drawback to PET, as noted earlier, is that subjects have to perform a task for roughly 40 seconds, rendering a temporal resolution in the tens of seconds. fMRI, on the other hand, has a resolution on the order of seconds for whole brain imaging. This temporal resolution for fMRI allows one to measure the effects of a series of single events with fMRI, whereas one can only measure long blocks of events with PET. Hence, many fMRI studies currently use event-related paradigms, which offer greater flexibility in experimental inquiry. PET is also at a disadvantage relative to fMRI in terms of spatial resolution. Nonetheless, one advantage that PET offers over fMRI is that it is not prone to the loss of signal near air-tissue interfaces, as is the case with BOLD-contrast fMRI. A second advantage is that the PET scanning environment suffers from less acoustic noise than the fMRI environment.

Musso et al. performed an interesting analogue study of aphasia rehabilitation with PET [63]. The authors performed 12 scans on each of 4 patients with Wernicke's aphasia performing a comprehension task. Between scans, they gave subjects intensive training in language comprehension that involved the use of linguistic and nonlinguistic cues in a variety of comprehension tasks. In addition to training in language comprehension, subjects received

a language comprehension test (Token Test) between the PET scans. Hence, performance on the Token Test could be correlated with voxel-wise values for rCBF at 12 different time points to determine if changes in performance correlated with changes in rCBF. Regions best correlated with training-induced improvement in verbal comprehension included the posterior right superior temporal gyrus and the left precuneus [63]. Findings were taken as an indication of participation of the right-hemisphere homologue of Wernicke's area in language comprehension gains.

Magnetoencephalography/Magnetic Source Imaging and Electroencephalography/Evoked Potentials

MEG and EEG represent two noninvasive functional brain imaging methods that work in a completely different manner than the earlier described functional imaging techniques (e.g., fMRI, PET). Both make use of the same neurophysiologic events, i.e., ionic currents caused by information exchange of neurons. Active neurons generate small, fluctuating electrical currents. During EEG, synchronized electrical activity of thousands of active neurons is detected by means of electrodes that are attached to the scalp. The electric currents inside the head also produce small magnetic field oscillations that are the sources of the MEG signal. The strength and orientation of these magnetic fields can be detected above the scalp by magnetometers inside the MEG system. Because the magnetic fields measured during MEG are very weak (i.e., a fraction of the of the Earth's magnetic field), it needs to be assessed within a magnetically shielded room by using specific recording devices that are sensitive to extremely small magnetic fields (superconducting quantum interference devices). As a result, MEG devices are extremely expensive (millions of dollars) while even advanced EEG systems are relatively inexpensive (several thousand dollars). EEG and MEG signals are mainly produced by postsynaptic ionic currents of synchroni-cally active pyramidal cortical neurons. But due to the properties of the neural sources of the respective signals that are measured during EEG and MEG (electric current flow vs magnetic fields that are oriented perpendicular to each other), EEG is most sensitive to activity generated on top of the cortical sulci, whereas MEG is more sensitive to activity in the sulci. Thus, both techniques can provide complementary information about neural activity [64].

Similar to other imaging techniques, spontaneous or evoked activity in response to specific behavior can be monitored (event-related electric potentials or event-related magnetic fields). In combination with anatomical information (e.g., structural MRI), both techniques allow one to estimate the underlying neuronal generators of the recorded surface activity by using complex mathematical procedures. The main advantage of electrophysiological techniques is that they can detect changes in brain activity with millisecond temporal resolution. Thus, EEG and MEG are the most direct correlates of online brain processing that can be obtained noninvasively. On the other hand, the spatial resolution is in the range of centimeters and thus lower than that obtained during fMRI. MEG offers slightly better spatial resolution than EEG, as the magnetic fields measured are not affected by the surrounding tissue [65].

Spontaneous neuroelectric or neuromagnetic activity in the healthy brain is characterized by rhythmic oscillatory activity in the frequency range above 8 Hz. Focal oscillations in lower frequency ranges (e.g., slow wave activity in the delta frequency range; 0.5–4.0 Hz) can be found in the vicinity of structural lesions (e.g., stroke, tumors) and have been interpreted as indicative of dysfunctional information processing capacity due to a loss of afferent input or due to a primary metabolic effect [66]. Mapping of slow-wave activity can help identify dysfunctional network characteristics in neuropsychiatric disorders or detect changes in brain activity over the course of recovery and in response to treatment [67]. For example, Lewine et al. demonstrated that improved neuropsychological functioning after traumatic brain injury was associated with reduced MEG-slow wave activity [68]. Hensel et al. reported reduced slow-wave activity to be associated with spontaneous recovery of language functions after stroke [69]. Moreover, improvement of language functions after speech and language therapy has been shown to covary with changes in delta

frequency in patients with stroke. Meinzer et al. [70] and De Jongh et al. [71] found reduced slow-wave activity after successful resection of brain tumors.

Due to the excellent temporal resolution, EEG and MEG have widely been used to detect spatiotemporal distribution in the brain of higher cognitive processes, like language functions. For example, during picture naming, visual and conceptual processes take place within the first 175 ms after stimulus presentation, followed by lexical retrieval (until ~250 ms) and phonological encoding of the word form (250–450 ms) [72], after neurological damage different aspects of word-retrieval can be impaired (e.g., post-stroke anomia). This has been shown by Laganaro et al., who used EEG to compare temporal characteristics of evoked responses during picture naming in patients with two different types of anomia [73]. Compared with a group of nondisabled subjects, the authors found early event-related potential abnormalities (100–250 ms) in patients with lexical-semantic impairments. In contrast, a group of patients with predominantly phonological impairments evidenced abnormalities in later time windows associated with phonological processing (300–450 ms). Electrophysiological techniques have also been used to track activity changes in response to treatment. For example, Cornelissen et al. assessed changes in brain activity after speech and language therapy that was designed to facilitate phonological encoding in patients with aphasia by means of MEG and MSI [74]. In line with studies in nondisabled subjects on phonological encoding, treatment-induced activity changes were found in the time window between 300 and 600 ms after picture presentation and were localized in the left inferior parietal cortex, an area associated with phonological encoding and storage [72].

More recently, researchers began to combine electrophysiological, blood flow-based techniques and structural imaging, because they provide converging lines of evidence to describe the neural substrates of normal cognitive functioning changes in pathological conditions, and to assess treatment-induced recovery of functions. For example, Meinzer et al. used MEG-slow wave mapping before a 2-week treatment period in poststroke aphasia to define areas of dysfunctional information processing [6]. Subsequently, slow-wave clusters were used as an ROI to assess functional activity changes in these brain areas with fMRI. Moreover, EEG can be assessed simultaneously during fMRI. In the future, the combination of these two methods could be useful for a better description of pathological processes or the effect of rehabilitation efforts. As in fMRI, MEG can be used to assess functional connections between different brain areas [75].

Near Infrared Spectroscopy

NIRS, like the various MR techniques, is a non-invasive method of looking at brain tissue function. Although visible light is strongly absorbed by various components in body tissue, light in the near infrared frequency range (650–900 nm) is less strongly absorbed and thus can penetrate through the skin and skull and a centimeter or two into the typical adult brain. In addition to being absorbed by tissue, light is strongly scattered. This further reduces the light intensity and penetration and hinders the ability to precisely localize absorbing species. However, the scattered light can be used to measure CBF.

Light absorption at a given wavelength follows the Beer-Lambert Law:

$$A_\lambda = \varepsilon_\lambda c l \ ,$$

where A = absorption, λ = wavelength, ε = absorption or molar extinction coefficient, c = molar concentration of the absorbing species, and l = optical path length. Molecules have different absorption spectra, which is the variability of the absorption coefficient with wavelength. The major species in tissue that absorb in the near infrared band and are present in significant quantities are cytochrome oxidase and hemoglobin, both of which exist in oxidized and reduced forms with unique absorption spectra.

It is possible to separately quantify the relative amounts of the reduced and oxidized forms of hemoglobin or cytochrome oxidase by using two measurement wavelengths (typically 760–780 nm for deoxyhemoglobin and 825–850 nm for oxyhemoglobin) at which the two forms have different

absorption coefficients. A separate measurement at an isosbestic point (815 nm for hemoglobin), a wavelength at which the absorption coefficients of the two species are equal, provides the total amount of reduced and oxidized forms, which is proportional to blood volume. From absorptions measured at these three wavelengths, the concentrations of both oxidized and reduced species are calculated. Thus NIRS can measure amounts of hemoglobin and deoxyhemoglobin in tissue, which BOLD fMRI cannot, because BOLD fMRI signal changes arise from a complex mixture of CBF, CBV, and oxygenation changes.

In practice, NIRS is applied in vivo by placing a light source and a light detector adjacent to each other above the region to be measured. The light path through the tissue between and below them, a convex banana-shaped tissue region, is sampled.

A combined NIRS-fMRI study of patients with middle cerebral artery stroke in chronic recovery compared with control subjects demonstrated ipsilateral motor cortex compensation in the patients with stroke [76]. NIRS monitoring of mechanically or therapist-assisted hemiplegic treadmill walking 3 months post-stroke showed stronger activation with therapist assistance and enhanced activation in the unaffected hemisphere [77]. A longitudinal study by the same group with NIRS monitoring at 3 and 5 months post-stroke showed decreased activation in the unaffected hemisphere and increased activation in the affected hemisphere in the second compared with the first session [78]; this shift towards normal lateralization has also been noted in fMRI studies of hand motor function. A similar trend towards increased, normal laterality was also noted in a longitudinal case study of NIRS monitoring of motor cortex activity during 10 consecutive days of constraint-induced movement therapy (CIMT) [79]. A Japanese group used NIRS to monitor brain effects of 13 rehabilitation tasks in patients with poststroke hemiplegia [80].

NIRS and transcranial Doppler ultrasound have been employed to monitor arterial blood flow and blood volume changes in response to hypercapnia in patients with lateralized stroke compared with non-disabled controls [81]. In the patients, NIRS showed an increase of blood volume with hypercapnia in the spared but not in the lesioned hemisphere. The two methods were also combined to monitor the effects of vinpocetine on CBF and oxyhemoglobin, deoxyhemoglobin, and total hemoglobin in the stroke-affected hemisphere [82]; vinpocetine increased both CBF and oxygen extraction.

Reviews of NIRS and BOLD fMRI studies of stroke and brain tumors [83] and of NIRS studies of stroke rehabilitation [84] provide an assessment of the opportunities and challenges. Strangman et al. also report results of test-retest reliability for NIRS [84].

In summary, NIRS has spatial resolution of slightly less than 1 cm, temporal resolution of milliseconds to tens of milliseconds, light penetration of only about 1 cm into the superficial portions of the brain, and the ability to estimate amounts of oxyhemoglobin, deoxyhemoglobin, and total hemoglobin. Thus, for superficial brain regions, it is a useful complement to fMRI. Its portability, relatively low cost compared with MR, ability to be used in a normal and unconfined environment, and noninvasiveness make it potentially useful clinically.

Transcranial Magnetic Stimulation

TMS is a painless, noninvasive neurophysiological technique during which a strong (typically 1–2 T) focal magnetic pulse is directed at cortical areas from a stimulation coil placed directly above the scalp. The brief (measured in microseconds) change in magnetic field induces a corresponding electrical potential change in the affected cortex, resulting in a rapid neuronal depolarization and the generation of action potentials. In the evaluation of the human motor system, typical output measures of TMS stimulation to the primary motor cortex (M_1) are changes in the electromyographs (EMG) of target muscles including, if the stimulation is properly applied, the generation of EMG activity spikes known as magnetic evoked potentials (MEPs). For the purposes of clinical research, TMS is typically delivered using one of three pulse (coil excitation) protocols: a single pulse, two pulses separated by a brief delay (paired pulse), or rapid repetitive pulses (repetitive TMS [rTMS]). The use of each within the domain of rehabilitative research will briefly be explored.

Single-pulse TMS, the oldest and most reported TMS procedure, refers to the application of a single

magnetic field change during stimulation trials. The technique has great clinical use as a diagnostic tool for the motor system. A prevalent single-pulse method in neurology is the assessment of an individual's central motor conduction time. In this procedure, a neurologist or technician uses single pulses to M_1 representations of different muscles throughout the arm and hand. Delays or alterations in the onset and latency of MEP spikes (from coil stimulation events) can determine if an individual with suspected pathology deviates from age-matched nondisabled values. Disorders such as MS, ALS, stroke, leukoaraiosis, and traumatic brain injury can all affect neural conduction rates from pyramidal cell impetus to the measured muscle actuation [85]. Another clinical use of single-pulse TMS is for mapping of the motor cortex. This approach is particularly useful in the assessment of cortical plasticity in both nondisabled and pathological states. During the mapping procedure, the location of greatest sensitivity (requiring least stimulator current to produce MEP) to a target muscle is first identified using a thresholding procedure [86]. After the "hotspot" is localized, stimulation proceeds at radially contiguous sites until the boundaries (areas that do not produce MEP) of the motor map are obtained. **Figure 7** shows data from our laboratory combining both fMRI and TMS motor maps. Rehabilitation research has made use of single-pulse cortical mapping to monitor change of maps over time in populations, including stroke [87–88], MS [89], Parkinson disease (PD) [90], ALS [91], and even polio [92].

Paired-pulse TMS is another technique that has been used in rehabilitation research. In a paired-pulse TMS paradigm, two pulses are delivered to the motor cortex, offset by a brief interstimulus interval. The initial pulse is called the conditioning pulse and is usually relative to the magnitude of current delivered to the coil during the second stimulation, which is called the test pulse. Researchers have discovered that variations in the temporal offset between the two pulses will alter the dynamics of the EMG output, as does variation of the relative magnetization strength between the conditioning and test stimulations. These changes can either produce a faciliatory or inhibitory effect deemed intracortical facilitation (ICF) or intracortical inhibition (ICI), respectively. Individuals with stroke [93–95] or PD [96] appear to exhibit deviations in levels of both ICF and ICI as compared with nondisabled adults. Interestingly, however, treatments such as CIMT in stroke [95] or stimulation of the subthalamic nucleus after deep brain stimulation [96] have shown positive effect in normalizing ICI and ICF.

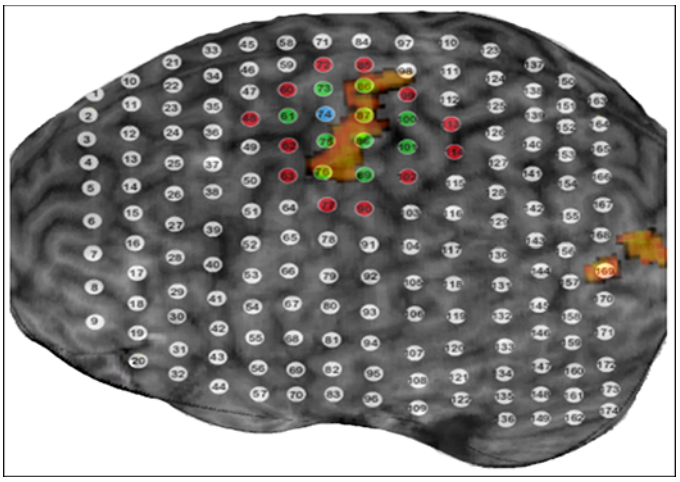

Figure 7.
Cortical motor map of first dorsal interosseous (FDI) muscle using single-pulse transcranial magnetic stimulation overlaid onto three-dimensional rendering of functional magnetic resonance imaging (fMRI) activation during FDI exercise. Site 74 (blue circle) represents cortical site of maximal sensitivity to FDI activation ("hotspot"). Green circles are areas that also generate magnetic evoked potential in target muscle, while red circles are map's boundary. Orange area represents active areas during fMRI at $F > 5.0$ ($p < 0.001$, uncorrected).

rTMS uses a train of TMS pulses delivered at either slow (1 Hz) or rapid (>1 Hz) frequencies to alter the firing patterns of affected cortex. Low frequency rTMS tends to depress the excitability of a target region, whereas high frequency has the opposite effect and tends to increase excitability in affected areas. As opposed to single- or paired-pulse TMS techniques, which are applied to the M_1 and whose output measures are change in EMG signal, rTMS can be applied to any accessible cortical region, including prefrontal, parietal, temporal or occipital areas. rTMS is being used with greater regularity as a treatment protocol for an increasing number of disorders. For example, in stroke recovery, Naeser et al.

used low frequency rTMS with patients afflicted with Broca's aphasia to improve naming ability without concomitant speech therapy [97]. rTMS has also been used in the treatment of depression [98], PD [99], chronic pain [100], dystonia [101], and schizophrenia [102], among many others.

Compared with other modalities of neurological research, TMS, as a technique, offers some significant advantages. Single- and paired-pulse TMS allows for direct inquiry into the activation of CST, and its measure (EMG change) can increase or decrease in magnitude relative to the amount of current applied through the magnetic coil. Conversely, fMRI and PET are indirect measures of neural activity that rely on correlates of blood flow to index activity relative to a comparison state. Measured responses in these modalities are therefore dependent on and limited by the dynamics of the human cerebrovascular system. The motor-related TMS procedures also benefit from the TMS's excellent temporal resolution in that MEP responses to TMS stimulation in target muscle typically occur from 18 to 30 ms after stimulation. Responses in imaging modalities are limited to seconds (fMRI) or tens of seconds (PET) to derive their respective responses. Finally, TMS offers great practical advantages over other modalities in that the typical TMS apparatus is both inexpensive (tens of thousands as compared with millions for fMRI, MEG, and PET) and quite portable (a single-pulse system easily fits on a small cart).

However, TMS is beset by some limitations as well. Primary amongst these is the fact that the magnetic fields produced by TMS coils can only show effects at a depth of <2 cm from the stimulation site. TMS can therefore only be used with cortical areas, whereas fMRI and PET can also be used to probe subcortical processes. A second limitation of TMS is its spatial resolution, which due to size of the delivery coil and the diffusion of the generated B_0, is limited to about 1 cm^2. Finally, great care has to be taken in the screening of participants and adherence to safety procedures because of the potential of headache and seizure from the stimulation, particularly for rTMS.

Given the strengths and limitations of TMS in comparison with imaging modalities, many researchers have begun to combine the neurophysiological technique with fMRI, particularly when using single- or paired-pulse designs. Our laboratory has combined the two techniques in the assessment of cortical maps of the FDI muscle (**Figure 7**). It is now possible to perform TMS stimulation while in the MRI scanner, a procedure being employed with greater frequency as the technology becomes more widely available [103].

CONCLUSIONS

The potential effect of functional neuroimaging for rehabilitation research, and ultimately for rehabilitation care, can hardly be overestimated. If functional neuroimaging can help define how brain systems reorganize during rehabilitation, designing treatments that enhance reorganization and thereby optimize rehabilitation may be possible. Further, functional imaging results may be found to predict rehabilitation outcome, including which treatments are optimal for patients with specific patterns of brain activity during tasks relevant to rehabilitation. Although the collection of a knowledge base adequate to affect clinical rehabilitation on a day-to-day basis may be years, or even decades away, important discoveries starting us down this path have already been made.

Advances in imaging over the past 2 or 3 decades have left rehabilitation investigators with a variety of tools to assess functional brain networks for behavior and cognition. These techniques include fMRI, PET, MEG, EEG, NIRS, and TMS, all of which we briefly discussed earlier. Each technique has strengths and weaknesses relating to cost, availability, temporal resolution, spatial resolution, and risk. For example, fMRI has become by far the most widely used technique for functional imaging because of its widespread availability, ability to perform structural images on the same acquisition platform as functional images, and excellent spatial resolution. However, fMRI does not have a temporal resolution capable of defining in real time the cascade of neuronal events in brain systems like EEG or MEG can and the widely used BOLD-contrast technique is vulnerable to signal loss near air-tissue interfaces. Although selection of an imaging technique for research is often a matter

of instrument availability and convenience, the kind of information necessary to answer experimental questions also should be given some consideration in designing rehabilitation studies. In addition to functional neuroimaging techniques, new developments in structural neuroimaging, i.e., the use of diffusion imaging techniques to define degree of white matter loss/integrity, can also enhance our understanding of substrates for rehabilitation.

Rehabilitation clinicians and rehabilitation researchers who do not participate in imaging research are consumers of neuroimaging research in rehabilitation. To be discerning consumers, they need some fundamental knowledge of functional neuroimaging techniques. We have tried not only to provide such fundamental information but also to refer the interested reader to additional sources of further information. The next decade or two is likely to bring important advances in our knowledge about brain systems, their plasticity, and their role in rehabilitation. Our ability to digest this information and use it in our clinical endeavors will enhance the lives of our patients.

Abbreviations: ALS = amyotrophic lateral sclerosis, ASL = arterial spin labeling, B_0 = magnetic field, BOLD = blood oxygenation level dependent, BOSS = blood oxygenation sensitive steady-state, CBF = cerebral blood flow, Cho = choline, CIMT = constraint-induced movement therapy, Cr = creatine, CSI = chemical shift imaging, CST = corticospinal tract, DCM = dynamic causal modeling, DSC = dynamic susceptibility contrast, DTI = diffusion tensor imaging, DW-MRI = diffusion-weighted magnetic resonance imaging, EEG = electroencephalography, EMG = electromyograph, FA = fractional anisotropy, fcMRI = functional-connectivity magnetic resonance imagining, FDG = fluorodeoxyglucose, fMRI = functional magnetic resonance imaging, ICF = intracortical facilitation, ICI = intracortical inhibition, L_1 = first language, L_2 = second language, Lac = lactate, M = magnetization, M_1 = primary motor cortex, MD = mean diffusivity, MEG = magnetoencephalography, MEP = magnetic evoked potential, MR = magnetic resonance, MRI = magnetic resonance imaging, MRS = magnetic resonance spectroscopy, MS = multiple sclerosis, MSI = magnetic source imaging, MT = magnetization transfer, NAA = N-acetylaspartate, NIRS = near infrared spectroscopy, NMR = nuclear magnetic resonance, PD = Parkinson disease, PDD = principle diffusion direction, PET = positron emission tomography, ppm = parts per million, rCBF = regional cerebral blood flow, rf = radiofrequency, ROI = region of interest, rTMS = repetitive transcranial magnetic stimulation, SEM = structural equation modeling, TE = echo time, TMS = transcranial magnetic stimulation, TR = repetition time.

ACKNOWLEDGMENTS

Funding/Support: This material was based on work supported by a Department of Veterans Affairs Rehabilitation Research and Development Senior Research Career Scientist Award to Dr. Crosson (grant B6364S); the Department of Veterans Affairs Rehabilitation Research and Development Service Center of Excellence (grant B6793C); the National Institute on Deafness and Other Communication Disorders (grants R01 DC007387 and R21 DC009247); the German Science Foundation (grant ME 3161/2-1); the Mobility Foundation Center, Dallas, Texas; and the U.S. Army Medical Research and Materiel Command (grant DAMD17-01-1-0741). The content of this article does not necessarily reflect the position or the policy of the U.S. government and no official endorsement should be inferred.

REFERENCES

1. Raichle ME. A brief history of human functional brain mapping. In: Toga AW, Mazziota JC, editors. Brain mapping: The systems. New York (NY): Academic Press; 2000. p. 33–75. DOI:10.1016/B978-012692545-6/50004-0
2. Metter EJ, Kempler D, Jackson C, Hanson WR, Mazziotta JC, Phelps ME. Cerebral glucose metabolism in Wernicke's, Broca's, and conduction aphasia. Arch Neurol. 1989;46(1):27–34. [PMID: 2783365]
3. Love T, Swinney D, Wong E, Buxton R. Perfusion imaging and stroke: A more sensitive measure of the brain bases of cognitive deficits. Aphasiology. 2002;16(9):873–83. DOI:10.1080/02687030244000356
4. Dobkin BH, Firestine A, West M, Saremi K, Woods R. Ankle dorsiflexion as an fMRI paradigm to assay motor control for walking during rehabilitation. Neuroimage. 2004;23(1):370–81. [PMID: 15325385] DOI:10.1016/j.neuroimage.2004.06.008
5. Breier JI, Castillo EM, Boake C, Billingsley R, Maher L, Francisco G, Papanicolaou AC. Spatiotemporal patterns of language-specific brain activity in patients with chronic aphasia after stroke using magnetoencephalography. Neuroimage. 2004;23(4):1308–16. [PMID: 15589095] DOI:10.1016/j.neuroimage.2004.07.069
6. Meinzer M, Flaisch T, Breitenstein C, Wienbruch C, Elbert T, Rockstroh B. Functional re-recruitment of dysfunctional brain areas predicts language recovery in chronic aphasia. Neuroimage. 2008;

39(4):2038–46. [PMID: 18096407] DOI:10.1016/j.neuroimage.2007.10.008

7. Peck KK, Wierenga CE, Moore AB, Maher LM, Gopinath K, Gaiefsky M, Briggs RW, Crosson B. Comparison of baseline conditions to investigate syntactic production using functional magnetic resonance imaging. Neuroimage. 2004;23(1):104–10. [PMID: 15325357] DOI:10.1016/j.neuroimage.2004.05.006
8. Newman SD, Twieg DB, Carpenter PA. Baseline conditions and subtractive logic in neuroimaging. Hum Brain Mapp. 2001;14(4):228–35. [PMID: 11668654] DOI:10.1002/hbm.1055
9. Petersen SE, Van Mier H, Fiez JA, Raichle ME. The effects of practice on the functional anatomy of task performance. Proc Natl Acad Sci U S A. 1998; 95(3):853–60. [PMID: 9448251] DOI:10.1073/pnas.95.3.853
10. Buxton R. Introduction to functional magnetic resonance imaging: Principles and techniques. New York (NY): Cambridge University Press; 2009.
11. Crosson B, McGregor K, Gopinath KS, Conway TW, Benjamin M, Chang YL, Moore AB, Raymer AM, Briggs RW, Sherod MG, Wierenga CE, White KD. Functional MRI of language in aphasia: A review of the literature and the methodological challenges. Neuropsychol Rev. 2007;17(2):157–77. [PMID: 17525865] DOI:10.1007/s11065-007-9024-z
12. Crosson B, Moore AB, McGregor KM, Chang YL, Benjamin M, Gopinath K, Sherod ME, Wierenga CE, Peck KK, Briggs RW, Rothi LJ, White KD. Regional changes in word-production laterality after a naming treatment designed to produce a rightward shift in frontal activity. Brain Lang. 2009;111(2):73–85. [PMID: 19811814] DOI:10.1016/j.bandl.2009.08.001
13. Crosson B, Fabrizio KS, Singletary F, Cato MA, Wierenga CE, Parkinson RB, Sherod ME, Moore AB, Ciampitti M, Holiway B, Leon S, Rodriguez A, Kendall DL, Levy IF, Rothi LJ. Treatment of naming in nonfluent aphasia through manipulation of intention and attention: A phase 1 comparison of two novel treatments. J Int Neuropsychol Soc. 2007;13(4):582–94. [PMID: 17521480] DOI:10.1017/S1355617707070737
14. Golay X, Hendrikse J, Lim TC. Perfusion imaging using arterial spin labeling. Top Magn Reson Imaging. 2004;15(1):10–27. [PMID: 15057170] DOI:10.1097/00002142-200402000-00003
15. Liu TT, Brown GG. Measurement of cerebral perfusion with arterial spin labeling: Part 1. Methods. J Int Neuropsychol Soc. 2007;13(3):517–25. [PMID: 17445301] DOI:10.1017/S1355617707070646
16. Parkes LM. Quantification of cerebral perfusion using arterial spin labeling: Two-compartment models. J Magn Reson Imaging. 2005;22(6):732–36. [PMID: 16267854] DOI:10.1002/jmri.20456
17. Wolff SD, Balaban RS. Magnetization transfer contrast (MTC) and tissue water proton relaxation in vivo. Magn Reson Med. 1989;10(1):135–44. [PMID: 2547135] DOI:10.1002/mrm.1910100113
18. Pollock JM, Deibler AR, Whitlow CT, Tan H, Kraft RA, Burdette JH, Maldjian JA. Hypercapnia-induced cerebral hyperperfusion: An underrecognized clinical entity. AJNR Am J Neuroradiol. 2009;30(2):378–85. [PMID: 18854443] DOI:10.3174/ajnr.A1316
19. MacIntosh BJ, Pattinson KT, Gallichan D, Ahmad I, Miller KL, Feinberg DA, Wise RG, Jezzard P. Measuring the effects of remifentanil on cerebral blood flow and arterial arrival time using 3D GRASE MRI with pulsed arterial spin labelling. J Cereb Blood Flow Metab. 2008;28(8):1514–22. [PMID: 18506198] DOI:10.1038/jcbfm.2008.46
20. Detre JA, Samuels OB, Alsop DC, Gonzalez-At JB, Kasner SE, Raps EC. Noninvasive magnetic resonance imaging evaluation of cerebral blood flow with acetazolamide challenge in patients with cerebrovascular stenosis. J Magn Reson Imaging. 1999;10(5): 870–75. [PMID: 10548801] DOI:10.1002/(SICI)1522-2586(199911)10:5<870::AID-JMRI36>3.0.CO;2-D
21. Kemeny S, Ye FQ, Birn R, Braun AR. Comparison of continuous overt speech fMRI using BOLD and arterial spin labeling. Hum Brain Mapp. 2005; 24(3):173–83. [PMID: 15486986] DOI:10.1002/hbm.20078
22. Brown GG, Clark C, Liu TT. Measurement of cerebral perfusion with arterial spin labeling: Part 2. Applications. J Int Neuropsychol Soc. 2007;13(3): 526–38. [PMID: 17445302] DOI:10.1017/S1355617707070634

23. Miller KL, Hargreaves BA, Lee J, Ress D, DeCharms RC, Pauly JM. Functional brain imaging with BOSS FMRI. Conf Proc IEEE Eng Med Biol Soc. 2004;7: 5234–37. [PMID: 17271520]
24. Miller KL, Hargreaves BA, Lee J, Ress D, DeCharms RC, Pauly JM. Functional brain imaging using a blood oxygenation sensitive steady state. Magn Res Med. 2003;50(4):675–83. [PMID: 14523951] DOI:10.1002/mrm.10602
25. Miller KL, Smith SM, Jezzard P, Pauly JM. High-resolution FMRI at 1.5T using balanced SSFP. Magn Res Med. 2006;55(1):161–70. [PMID: 16345040] DOI:10.1002/mrm.20753
26. Naeser MA, Martin PI, Baker EH, Hodge SM, Sczerzenie SE, Nicholas M, Palumbo CL, Goodglass H, Wingfield A, Samaraweera R, Harris G, Baird A, Renshaw P, Yurgelun-Todd D. Overt propositional speech in chronic nonfluent aphasia studied with the dynamic susceptibility contrast fMRI method. Neuroimage. 2004;22(1):29–41. [PMID: 15109995] DOI:10.1016/j.neuroimage.2003.11.016
27. Glover GH, Li TQ, Ress D. Image-based method for retrospective correction of physiological motion effects in fMRI; RETOICOR. Magn Reson Med. 2000;44(1):162–67. [PMID: 10893535] DOI:10.1002/1522-2594(200007)44:1<162::AID-MRM23>3.0.CO;2-E
28. Thomason ME, Foland LC, Glover GH. Calibration of BOLD fMRI using breath holding reduces group variance during a cognitive task. Hum Brain Mapp. 2007;28(1):59–68. [PMID: 16671081] DOI:10.1002/hbm.20241
29. Biswal BB, Kannurpatti SS, Rypma B. Hemodynamic scaling of fMRI-BOLD signal: Validation of low-frequency spectral amplitude as a scalability factor. Magn Reson Imaging. 2007;25(10):1358–69. [PMID: 17482411] DOI:10.1016/j.mri.2007.03.022
30. De Luca M, Beckmann CF, De Stefano N, Matthews PM, Smith SM. fMRI resting state networks define distinct modes of long-distance interactions in the human brain. Neuroimage. 2006;29(4):1359–67. [PMID: 16260155] DOI:10.1016/j.neuroimage.2005.08.035
31. Di Martino A, Scheres A, Margulies DS, Kelly AM, Uddin LQ, Shehzad Z, Biswal B, Walters JR, Castellanos FX, Milham MP. Functional connectivity of human striatum: A resting state fMRI study. Cereb Cortex. 2008;18(12):2735–47. [PMID: 18400794] DOI:10.1093/cercor/bhn041
32. Schoenfeld MA, Noesselt T, Poggel D, Tempelmann C, Hopf JM, Woldorff MG, Heinze HJ, Hillyard SA. Analysis of pathways mediating preserved vision after striate cortex lesions. Ann Neurol. 2002; 52(6):814–24. [PMID: 12447936] DOI:10.1002/ana.10394
33. He BJ, Snyder AZ, Vincent JL, Epstein A, Shulman GL, Corbetta M. Breakdown of functional connectivity in frontoparietal networks underlies behavioral deficits in spatial neglect. Neuron. 2007; 53(6):905–18. [PMID: 17359924] DOI:10.1016/j.neuron.2007.02.013
34. Damoiseaux JS, Greicius MD. Greater than the sum of its parts: A review of studies combining structural connectivity and resting-state functional connectivity. Brain Struct Funct. 2009;213(6):525–33. [PMID: 19565262] DOI:10.1007/s00429-009-0208-6
35. Gerloff C, Bushara K, Sailer A, Wassermann EM, Chen R, Matsuoka T, Waldvogel D, Wittenberg GF, Ishii K, Cohen LG, Hallett M. Multimodal imaging of brain reorganization in motor areas of the contralesional hemisphere of well recovered patients after capsular stroke. Brain. 2006;129(Pt 3):791–808. [PMID: 16364955] DOI:10.1093/brain/awh713
36. Meister IG, Sparing R, Foltys H, Gebert D, Huber W, Töpper R, Boroojerdi B. Functional connectivity between cortical hand motor and language areas during recovery from aphasia. J Neurol Sci. 2006; 247(2):165–68. [PMID: 16737714 DOI:10.1016/j.jns.2006.04.003
37. Abutalebi J, Rosa PA, Tettamanti M, Green DW, Cappa SF. Bilingual aphasia and language control: A follow-up fMRI and intrinsic connectivity study. Brain Lang. 2009;109(2–3):141–56. [PMID: 19427522] DOI:10.1016/j.bandl.2009.03.003
38. Basser PJ, Mattiello J, LeBihan D. MR diffusion tensor spectroscopy and imaging. Biophys J. 1994; 66(1):259–67. [PMID: 8130344] DOI:10.1016/S0006-3495(94)80775-1
39. O'Sullivan M, Summers PE, Jones DK, Jarosz JM, Williams SC, Markus HS. Normal-appearing white matter in ischemic leukoaraiosis: A diffusion tensor MRI study. Neurology. 2001;57(12):2307–10. [PMID: 11756617]

40. Thomalla G, Glauche V, Koch MA, Beaulieu C, Weiller C, Röther J. Diffusion tensor imaging detects early Wallerian degeneration of the pyramidal tract after ischemic stroke. Neuroimage. 2004; 22(4):1767–74. [PMID: 15275932] DOI:10.1016/j.neuroimage.2004.03.041
41. Ciccarelli O, Behrens TE, Johansen-Berg H, Talbot K, Orrell RW, Howard RS, Nunes RG, Miller DH, Matthews PM, Thompson AJ, Smith SM. Investigation of white matter pathology in ALS and PLS using tract-based spatial statistics. Human Brain Mapp. 2009;30(2):615–24. [PMID: 18172851] DOI:10.1002/hbm.20527
42. Smith SM, Johansen-Berg H, Jenkinson M, Rueckert D, Nichols TE, Miller KL, Robson MD, Jones DK, Klein JC, Bartsch AJ, Behrens TE. Acquisition and voxelwise analysis of multi-subject diffusion data with tract-based spatial statistics. Nat Protoc. 2007;2(3):499–503. [PMID: 17406613] DOI:10.1038/nprot.2007.45
43. Bengtsson SL, Nagy Z, Skare S, Forsman L, Forssberg H, Ullén F. Extensive piano practicing has regionally specific effects on white matter development. Nature Neurosci. 2005;8(9):1148–50. [PMID: 16116456] DOI:10.1038/nn1516
44. Douaud G, Behrens TE, Poupon C, Cointepas Y, Jbabdi S, Gaura V, Golestani N, Krystkowiak P, Verny C, Damier P, Bachoud-Lévi AC, Hantraye P, Remy P. In vivo evidence for the selective subcortical degeneration in Huntington's disease. Neuroimage. 2009;46(4):958–66. [PMID: 19332141] DOI:10.1016/j.neuroimage.2009.03.044
45. Nelles M, Gleseke J, Flacke S, Lachenmayer L, Schild HH, Urbach H. Diffusion tensor pyramidal tractography in patients with anterior choroidal artery infarcts. Am J Neuroradiol. 2008;29(3):488–93. [PMID: 18079190] DOI:10.3174/ajnr.A0855
46. Ciccarelli O, Behrens TE, Altmann DR, Orrell RW, Howard RS, Johansen-Berg H, Miller DH, Matthews PM, Thompson AJ. Probabilistic diffusion tractography: A potential tool to assess the rate of disease progression in amyotrophic lateral sclerosis. Brain. 2006;129(Pt 7):1859–71. [PMID: 16672290] DOI:10.1093/brain/awl100
47. Govindaraju V, Young K, Maudsley AA. Proton NMR chemical shifts and coupling constants for brain metabolites. NMR Biomed. 2000;13(3):129–53. [PMID: 10861994] DOI:10.1002/1099-1492(200005)13:3<129::AID-NBM619>3.0.CO;2-V
48. Gideon P, Henriksen O, Sperling B, Christiansen P, Olsen TS, Jørgensen HS, Arlien-Søborg P. Early time course of N-acetylaspartate, creatine and phosphocreatine, and compounds containing choline in the brain after acute stroke. A proton magnetic resonance spectroscopy study. Stroke. 1992;23(11): 1566–72. [PMID: 1440704]
49. Saunders DE. MR spectroscopy in stroke. Br Med Bull. 2000;56(2):334–45. [PMID: 11092084] DOI:10.1258/0007142001903256
50. Brulatout S, Méric P, Loubinoux I, Borredon J, Corrèze JL, Roucher P, Gillet B, Bérenger G, Beloeil JC, Tiffon B, Mispelter J, Seylaz J. A one-dimensional (proton and phosphorus) and two-dimensional (proton) in vivo NMR spectroscopic study of reversible global cerebral ischemia. J Neurochem. 1996;66(6):2491–99. [PMID: 8632174]
51. De Stefano N, Matthews PM, Arnold DL. Reversible decreases in N-acetylaspartate after acute brain injury. Magn Reson Med. 1995;34(5):721–27. [PMID: 8544693] DOI:10.1002/mrm.1910340511
52. Eliassen JC, Boespflug EL, Lamy M, Allendorfer J, Chu WJ, Szaflarski JP. Brain-mapping techniques for evaluating poststroke recovery and rehabilitation: A review. Top Stroke Rehabil. 2008;15(5): 427–50. [PMID: 19008203] DOI:10.1310/tsr1505-427
53. Mountz JM. Nuclear medicine in the rehabilitative treatment evaluation in stroke recovery. Role of diaschisis resolution and cerebral reorganization. Eura Medicophys. 2003;43(2):221–39. [PMID: 17268387]
54. Moffett JR, Ross B, Arun P, Madhavarao CN, Namboodiri AM. N-Acetylaspartate in the CNS: From neurodiagnostics to neurobiology. Prog Neurobiol. 2007;81(2):89–131. [PMID: 17275978] DOI:10.1016/j.pneurobio.2006.12.003
55. Rudkin TM, Arnold DL. Proton magnetic resonance spectroscopy for the diagnosis and management of cerebral disorders. Arch Neurol. 1999; 56(8):919–26. [PMID: 10448796] DOI:10.1001/archneur.56.8.919
56. Graham GD, Blamire AM, Howseman AM, Rothman DL, Fayad PB, Brass LM, Petroff OA, Shulman

RG, Prichard JW. Proton magnetic resonance spectroscopy of cerebral lactate and other metabolites in stroke patients. Stroke. 1992;23(3):333–40. [PMID: 1542892]

57. Gillard JH, Waldman AD, Barker PB. Clinical MR neuroimaging: Diffusion, perfusion, and spectroscopy. New York (NY): Cambridge University Press; 2005.
58. Provencher SW. Estimation of metabolite concentrations from localized in vivo proton NMR spectra. Magn Reson Med. 1993;30(6):672–79. [PMID: 8139448] DOI:10.1002/mrm.1910300604
59. Ernst TR, Kreis R, Ross BD. Absolute quantitation of water and metabolites in the human brain. I: Compartments and water. J Magn Reson Ser B. 1993;102(1):1–8. DOI:10.1006/jmrb.1993.1055
60. Kreis R, Ernst T, Ross BD. Absolute quantitation of water and metabolites in the human brain. II. Metabolite concentrations. J Magn Reson Ser B. 1993;102(1):9–19. DOI:10.1006/jmrb.1993.1056
61. Barker PB, Soher BJ, Blackband SJ, Chatham JC, Mathews VP, Bryan RN. Quantitation of proton NMR spectra of the human brain using tissue water as an internal concentration reference. NMR Biomed. 1993;6(1):89–94. [PMID: 8384470] DOI:10.1002/nbm.1940060114
62. Träber F, Block W, Lamerichs R, Gieseke J, Schild HH. 1H metabolite relaxation times at 3.0 tesla: Measurements of T1 and T2 values in normal brain and determination of regional differences in transverse relaxation. J Magn Reson Imaging. 2004; 19(5):537–45. [PMID: 15112302] DOI:10.1002/jmri.20053
63. Musso M, Weiller C, Kiebel S, Muller SP, Bülau P, Rijntjes M. Training-induced brain plasticity in aphasia. Brain. 1999;122(Pt 9):1781–90. [PMID: 10468516] DOI:10.1093/brain/122.9.1781
64. Babiloni C, Pizzella V, Gratta CD, Ferretti A, Romani GL. Fundamentals of electroencefalography, magnetoencefalography, and functional magnetic resonance imaging. Int Rev Neurobiol. 2009; 86:67–80. [PMID: 19607991] DOI:10.1016/S0074-7742(09)86005-4
65. Johnsrude I, Hauk O. Neuroimaging: Techniques for examining human brain function. In: Braisby N, editor. Cognitive psychology: A methods companion. New York (NY): Oxford University Press; 2005.
66. Kamada K, Saguer M, Möller M, Wicklow K, Katenhäuser M, Kober H, Vieth J. Functional and metabolic analysis of cerebral ischemia using magnetoencephalography and proton magnetic resonance spectroscopy. Ann Neurol. 1997;42(4):554–63. [PMID: 9382466] DOI:10.1002/ana.410420405
67. Weisz N, Moratti S, Meinzer M, Dohrmann K, Elbert T. Tinnitus perception and distress is related to abnormal spontaneous brain activity as measured by magnetoencephalography. PLoS Med. 2005;2(6):e153. [PMID: 15971936] DOI:10.1371/journal.pmed.0020153
68. Lewine JD, Davis JT, Sloan JH, Kodituwakku PW, Orrison WW Jr. Neuromagnetic assessment of pathophysiologic brain activity induced by minor head trauma. AJNR Am J Neuroradiol. 1999;20(5): 857–66. [PMID: 10369357]
69. Hensel S, Rockstroh B, Berg P, Elbert T, Schönle PW. Left-hemispheric abnormal EEG activity in relation to impairment and recovery in aphasic patients. Psychophysiology. 2004;41(3):394–400. [PMID: 15102124] DOI:10.1111/j.1469-8986.2004.00164x
70. Meinzer M, Elbert T, Wienbruch C, Djundja D, Barthel G, Rockstroh B. Intensive language training enhances brain plasticity in chronic aphasia. BMC Biol. 2004;2:20. [PMID: 15331014] DOI:10.1186/1741-7007-2-20
71. De Jongh A, De Munck JC, Baayen JC, Puligheddu M, Jonkman EJ, Stam CJ. Localization of fast MEG waves in patients with brain tumors and epilepsy. Brain Topogr. 2003;15(3):173–79. [PMID: 12705813] DOI:10.1023/A:1022658217474
72. Indefrey P, Levelt WJ. The spatial and temporal signatures of word production components. Cognition. 2004;92(1–2):101–44. [PMID: 15037128] DOI:10.1016/j.cognition.2002.06.001
73. Laganaro M, Morand S, Schwitter V, Zimmermann C, Camen C, Schnider A. Electrophysiological correlates of different anomic patterns in comparison with normal word production. Cortex. 2009; 45(6):697–707. [PMID: 19103446] DOI:10.1016/j.cortex.2008.09.007
74. Cornelissen K, Laine M, Tarkiainen A, Järvensivu T, Martin N, Salmelin R. Adult brain plasticity elicited

by anomia treatment. J Cogn Neurosci. 2003;15(3): 444–61. [PMID: 12729495] DOI:10.1162/089892903321593153

75. Schlee W, Mueller N, Hartmann T, Keil J, Lorenz I, Weisz N. Mapping cortical hubs in tinnitus. BMC Biol. 2009;7:80. [PMID: 19930625] DOI:10.1186/1741-7007-7-80
76. Kato H, Izumiyama M, Koizumi H, Takahashi A, Itoyama Y. Near-infrared spectroscopic topography as a tool to monitor motor reorganization after hemiparetic stroke: A comparison with functional MRI. Stroke. 2002;33(8):2032–36. [PMID: 12154258] DOI:10.1161/01.STR.0000021903.52901.97
77. Miyai I, Yagura H, Oda I, Konishi I, Eda H, Suzuki T, Kubota K. Premotor cortex is involved in restoration of gait in stroke. Ann Neurol. 2002;52(2): 188–94. [PMID: 12210789] DOI:10.1002/ana.10274
78. Miyai I, Yagura H, Hatakenaka M, Oda I, Konishi I, Kubota K. Longitudinal optical imaging study for locomotor recovery after stroke. Stroke. 2003; 34(12):2866–70. [PMID: 14615624] DOI:10.1161/01.STR.0000100166.81077.8A
79. Park SW, Butler AJ, Cavalheiro V, Alberts JL, Wolf SL. Changes in serial optical topography and TMS during task performance after constraint-induced movement therapy in stroke: A case study. Neurorehabil Neural Repair. 2004;18(2):95–105. [PMID: 15228805] DOI:10.1177/0888439004265113
80. Saitou H, Yanagi H, Hara S, Tsuchiya S, Tomura S. Cerebral blood volume and oxygenation among post-stroke hemiplegic patients: Effects of 13 rehabilitation tasks measured by near-infrared spectroscopy. Arch Phys Med Rehabil. 2000;81(10):1348–56. [PMID: 11030500] DOI:10.1053/apmr.2000.9400
81. Vernieri F, Rosato N, Pauri F, Tibuzzi F, Passarelli F, Rossini PM. Near infrared spectroscopy and transcranial Doppler in monohemispheric stroke. Eur Neurol. 1999;41(3):159–62. [PMID: 10202248] DOI:10.1159/000008041
82. Bönöczk P, Panczel G, Nagy Z. Vinpocetine increases cerebral blood flow and oxygenation in stroke patients: A near infrared spectroscopy and transcranial Doppler study. Eur J Ultrasound. 2002; 15(1–2):85–91. [PMID: 12044859]
83. Sakatani K, Murata Y, Fujiwara N, Hoshino T, Nakamura S, Kano T, Katayama Y. Comparison of blood-oxygen-level–dependent functional magnetic resonance imaging and near-infrared spectroscopy recording during functional brain activation in patients with stroke and brain tumors. J Biomed Optics. 2007;12(6):062110. [PMID: 18163813] DOI:10.1117/1.2823036
84. Strangman G, Goldstein R, Rauch SL, Stein J. Near-infrared spectroscopy and imaging for investigating stroke rehabilitation: Test-retest reliability and review of the literature. Arch Phys Med Rehabil. 2006;87(12 Suppl 2):S12–S19. [PMID: 17140875] DOI:10.1016/j.apmr.2006.07.269
85. Chen R, Cros D, Curra A, Di Lazzaro V, Lefaucheur JP, Magistris MR, Mills K, Rösler KM, Triggs WJ, Ugawa Y, Ziemann U. The clinical diagnostic utility of transcranial magnetic stimulation: Report of an IFCN committee. Clin Neurophysiol. 2008;119(3): 504–32. [PMID: 18063409] DOI:10.1016/j.clinph.2007.10.014
86. Kleim JA, Kleim ED, Cramer SC. Systematic assessment of training-induced changes in corticospinal output to hand using frameless stereotaxic transcranial magnetic stimulation. Nat Protoc. 2007;2(7):1675–84. [PMID: 17641632] DOI:10.1038/nprot.2007.206
87. Butler AJ, Kahn S, Wolf SL, Weiss P. Finger extensor variability in TMS parameters among chronic stroke patients. J Neuroeng Rehabil. 2005;2:10. [PMID: 15927075] DOI:10.1186/1743-0003-2-10
88. Foltys H, Krings T, Meister IG, Sparing R, Boroojerdi B, Thron A, Töpper R. Motor representation in patients rapidly recovering after stroke: A functional magnetic resonance imaging and transcranial magnetic stimulation study. Clin Neurophysiol. 2003; 114(12):2404–15. [PMID: 14652101] DOI:10.1016/S1388-2457(03)00263-3
89. Thickbroom GW, Byrnes ML, Archer SA, Kermode AG, Mastaglia FL. Corticomotor organisation and motor function in multiple sclerosis. J Neurol. 2005;252(7):765–71. [PMID: 15750708] DOI:10.1007/s00415-005-0728-9
90. Filippi MM, Oliveri M, Pasqualetti P, Cicinelli P, Traversa R, Vernieri F, Palmieri MG, Rossini PM. Effects of motor imagery on motor cortical output

topography in Parkinson's disease. Neurology. 2001;57(1):55–61. [PMID: 11445628]

91. De Carvalho M, Miranda PC, Luís ML, Ducla-Soares E. Cortical muscle representation in amyotrophic lateral sclerosis patients: Changes with disease evolution. Muscle Nerve. 1999;22(12):1684–92. [PMID: 10567081] DOI:10.1002/(SICI)1097-4598(199912)22:12<1684::AID-MUS10>3.0.CO;2-X

92. Oliveri M, Brighina F, La Bua V, Buffa D, Aloisio A, Fierro B. Reorganization of cortical motor area in prior polio patients. Clin Neurophysiol. 1999; 110(5):806–12. [PMID: 10400193] DOI:10.1016/S1388-2457(98)00055-8

93. Manganotti P, Acler M, Zanette GP, Smania N, Fiaschi A. Motor cortical disinhibition during early and late recovery after stroke. Neurorehabil Neural Repair. 2008;22(4):396–403. [PMID: 18326890] DOI:10.1177/1545968307313505

94. Swayne OB, Rothwell JC, Ward NS, Greenwood RJ. Stages of motor output reorganization after hemispheric stroke suggested by longitudinal studies of cortical physiology. Cereb Cortex. 2008; 18(8):1909–22. [PMID: 18234688] DOI:10.1093/cercor/bhm218

95. Liepert J. Motor cortex excitability in stroke before and after constraint-induced movement therapy. Cogn Behav Neurol. 2006;19(1):41–47. [PMID: 16633018] DOI:10.1097/00146965-200603000-00005

96. Däuper J, Peschel T, Schrader C, Kohlmetz C, Joppich G, Nager W, Dengler R, Rollnik JD. Effects of subthalamic nucleus (STN) stimulation on motor cortex excitability. Neurology. 2002;9(5):700–706. [PMID: 12221160]

97. Naeser MA, Martin PI, Nicholas M, Baker EH, Seekins H, Kobayashi M, Theoret H, Fregni F, Maria-Tormos J, Kurland J, Doron KW, Pascual-Leone A. Improved picture naming in chronic aphasia after TMS to part of right Broca's area: An open-protocol study. Brain Lang. 2005;93(1):95–105. [PMID: 15766771] DOI:10.1016/j.bandl.2004.08.004

98. Paus T, Barrett J. Transcranial magnetic stimulation (TMS) of the human frontal cortex: Implications for repetitive TMS treatment of depression. J Psychiatry Neurosci. 2004;29(4):268–79. [PMID: 15309043]

99. Lefaucheur JP. Repetitive transcranial magnetic stimulation (rTMS): Insights into the treatment of Parkinson's disease by cortical stimulation. Neurophysiol Clin. 2006;36(3):125–33. [PMID: 17046607] DOI:10.1016/j.neucli.2006.08.003

100. Leo RJ, Latif T. Repetitive transcranial magnetic stimulation (rTMS) in experimentally induced and chronic neuropathic pain: A review. J Pain. 2007; 8(6):453–59. [PMID: 17434804] DOI:10.1016/j.jpain.2007.01.009

101. Lefaucheur JP. Transcranial magnetic stimulation in the management of pain. Suppl Clin Neurophysiol. 2004;57:737–48. [PMID: 16106677] DOI:10.1016/S1567-424X(09)70415-5

102. Fitzgerald PB, Daskalakis ZJ. A review of repetitive transcranial magnetic stimulation use in the treatment of schizophrenia. Can J Psychiatry. 2008; 53(9):567–76. [PMID: 18801219]

103. Bohning DE, Shastri A, Nahas Z, Lorberbaum JP, Andersen SW, Dannels WR, Haxthausen EU, Vincent DJ, George MS. Echoplanar BOLD fMRI of brain activation induced by concurrent transcranial magnetic stimulation. Invest Radiol. 1998;33(6): 336–40. [PMID: 9647445] DOI:10.1097/00004424-199806000-00004

Bruce Crosson, PhD;[1–2]* Anastasia Ford, BS;[3] Keith M. McGregor, PhD;[1,3] Marcus Meinzer, PhD;[2] Sergey Cheshkov, PhD;[4] Xiufeng Li, PhD;[4] Delaina Walker-Batson, PhD;[5] Richard W. Briggs, PhD[4]

[1]Department of Veterans Affairs (VA) Rehabilitation Research and Development Brain Rehabilitation Research Center, Malcom Randall VA Medical Center, Gainesville, FL; Departments of [2]Clinical and Health Psychology and [3]Psychology, University of Florida, Gainesville, FL; [4]Department of Radiology, University of Texas Southwestern Medical Center, Dallas, TX; [5]The Stroke Center–Dallas, Texas Woman's University, Dallas, TX

[*]Email: nossorc1@phhp.ufl.edu

DOI:10.1682/JRRD.2010.02.0017